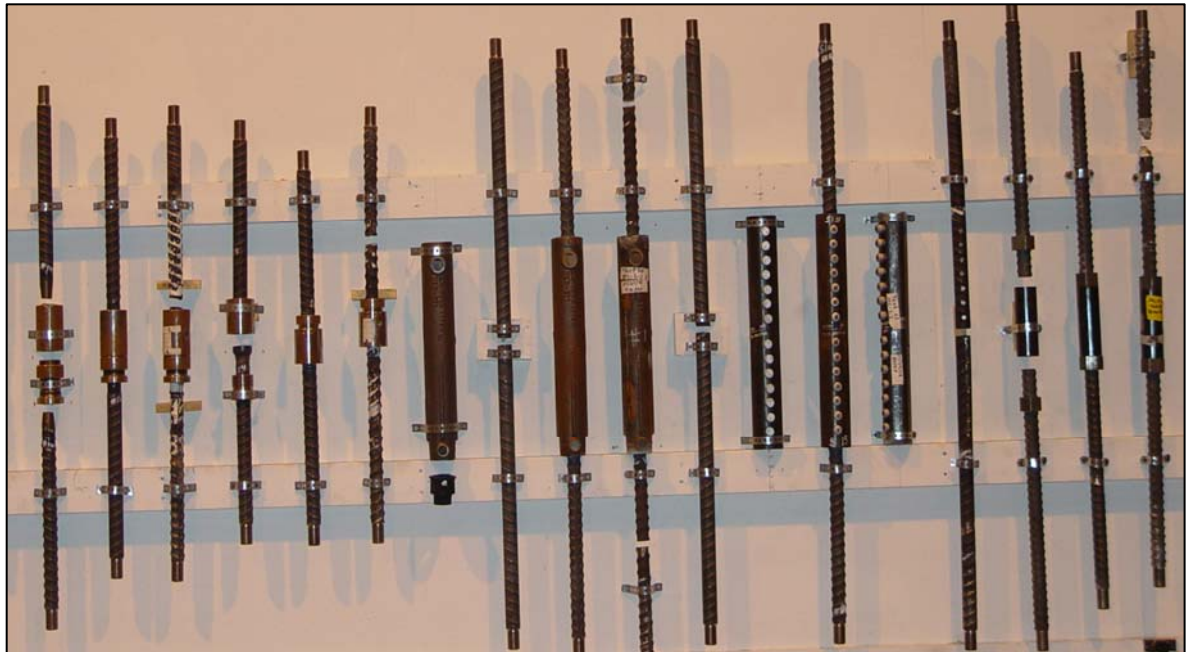Geotechnical and Structures Laboratory

US Army Corps of Engineers®
Engineer Research and Development Center

High Strain-Rate Testing of Mechanical Couplers

Stephen P. Rowell, Clifford E. Grey,
Stanley C. Woodson, and Kevin P. Hager

September 2009

High Strain-Rate Testing of Mechanical Couplers

Stephen P. Rowell and Stanley C. Woodson

Geotechnical and Structures Laboratory
U.S. Army Engineer Research and Development Center
3909 Halls Ferry Road
Vicksburg, MS 39180-6199

Clifford E. Grey

Information Technology Laboratory
U.S. Army Engineer Research and Development Center
3909 Halls Ferry Road
Vicksburg, MS 39180-6199

Kevin P. Hager

Naval Facilities Engineering Service Center
1100 23rd Avenue, Waterfront Structures Division
Port Hueneme, CA 93043

Final report

Abstract: Criteria for designing structures to resist the effects of accidental explosions are defined by Army Technical Manual (TM) 5-1300. These structures are built using steel-reinforced concrete. The current practice of splicing the flexural reinforcing steel is to lap the steel, which often creates a congestion of the steel in floors, walls, and adjoining corners. In 1971, a limited number of types of splices were tested at the U.S. Army Engineer Research and Development Center (ERDC) (formerly Waterways Experiment Station) to determine their performance under dynamic load conditions. Since then, several types of mechanical couplers have been tested and validated in developing the strength of reinforcing steel for cyclic loading and at strain rates expected during earthquakes. However, no mechanical couplers have been shown to meet the TM 5-1300 requirements. Therefore, five types of these modern mechanical couplers were selected and tested at the high strain rates expected during structural response to blast loads. This report focuses on the performance of the mechanical couplers at high strain rates.

Contents

Figures and Tables

Figures

Tables

Preface

The study reported herein was performed by staff members of the Structural Mechanics Branch (SMB) and the Research Group of the Geosciences and Structures Division (GSD), Geotechnical and Structures Laboratory (GSL), U.S. Army Engineer Research and Development Center (ERDC), along with personnel of the Sensors, Measurements, and Instrumentation Branch (SMI), Computational Science and Engineering Division (CSE), ERDC Information and Technology Laboratory (ITL). The investigation was sponsored by the Naval Facilities Engineering Service Center, Waterfront Structures Division (WSD). Kevin Hager was the WSD Project Engineer.

The Principal Investigator for this study was Stephen P. Rowell, GSD. Clifford E. Grey supervised all instrumentation and data collection. Dr. Stanley C. Woodson served as the technical subject matter expert. Frank D. Dallriva was Chief, SMB; Dr. Robert L. Hall was Chief, GSD; Dr. William P. Grogan was Deputy Director, GSL; and Dr. David W. Pittman was Director, GSL. Bruce C. Barker was Chief, SMI; Dr. Robert M. Wallace was Chief, CSE; Dr. Deborah F. Dent was Deputy Director, ITL; and Dr. Reed L. Mosher was Director, ITL.

COL Gary E. Johnston was Commander and Executive Director of ERDC. Dr. James R. Houston was Director.

Unit Conversion Factors

Multiply	By	To Obtain
degrees (angle)	0.01745329	radians
feet	0.3048	meters
inches	0.0254	meters
inch-pounds (force)	0.1129848	newton meters
pounds (force)	4.448222	newtons
pounds (force) per square inch	6.894757	kilopascals
pounds (mass)	0.45359237	kilograms
square inches	6.4516 E-04	square meters

1 Introduction

Background

Based on new security requirements, ordnance storage and maintenance facilities must be hardened and buried. Depending on the operational requirements, the cost of construction for modifying ordnance facilities may vary significantly. The total infrastructure cost for new construction and facility modification to support the Department of Defense will exceed $1 billion dollars. New facilities include magazines for long-term storage of ordnance and operational facilities for periodic inspection, maintenance, and life-extension of different weapons systems.

These facilities will be constructed using reinforced concrete to resist physical security threats and the effects of internal and external explosions. Department of the Army criteria for designing structures to resist the effects of accidental explosions or conventional weapons are defined by Technical Manual (TM) 5-1300 (Department of the Army et al. 1990) and TM 5-855-1 (Department of the Army et al. 1998), respectively. For accidental explosions, TM 5-1300 defines design methods applied to facilities used in the production, storage, and maintenance of ordnance and explosive materials. For conventional weapons effects, TM 5-855-1 defines design criteria for fixed, hardened structures.

Economic design of blast-resistant, reinforced concrete structures typically allows plastic deformations of the structural elements, which develops the ultimate strength and ductility of the steel reinforcement. Typical design details recommended in TM 5-1300 and TM 5-855-1 result in congestion of steel in slabs and beams and at corners. This congestion increases construction costs and difficulty in placing concrete between steel reinforcement bars. Figure 1 shows flexural and tension reinforcement at the corner between two walls. Standard hooks used to develop the strength of the flexural steel are also shown. Figure 2 shows flexural, diagonal shear, and direct shear reinforcement at the corner between a floor slab and a wall. Both figures illustrate the congestion of reinforcement at corners.

Figure 1. Flexural and tension steel reinforcement at a wall-to-wall corner.

Figure 2. Flexural, direct shear, and diagonal shear steel reinforcement.

TM 5-1300 allows the use of mechanical couplers to splice flexural steel reinforcement. However, the mechanical coupler must develop the ultimate dynamic tensile strength and ductility of the steel reinforcement. High strain-rate tension tests of the splice must be conducted to validate the performance of the splice. TM 5-855-1 allows the use of mechanical

couplers if the dynamic response of steel reinforcement to blast loads remains elastic.

In 1971, Cadweld, Thermite, and butt-welded splices were tested (Flathau 1971). Number 11 (1-3/8-in. diameter) reinforcing steel bars were tested at strain rates ranging from 0.05 to 3.0 sec^{-1}. Based on these tests, Cadweld and Thermite splices may be used in blast-resistant structures.

For structures in high seismic regions, mechanical couplers were developed to solve problems with steel congestion. Several manufacturers offer couplers that were tested and validated to develop the strength of reinforcing steel for cyclic loading and strain rates expected during earthquakes. However, no tests of these new mechanical couplers loaded at the high strain rates expected during blast loads have been documented. In addition, no open test standard has been developed for industry to test candidate splicing systems. Any open standard should provide a low-cost and rapid method for validating the behavior of mechanical splices at high strain rates.

Objective

The primary objective of the research reported herein was to measure the performance of mechanical couplers for splicing flexural reinforcing steel when stressed at high strain rates. Results of the testing may qualify commercially available mechanical couplers for use in blast-hardened structures. The secondary objective was to develop and document a preliminary open-source test procedure for testing mechanical couplers subjected to high strain-rate load conditions. This procedure will allow commercial vendors to test their products according to a defined standard and will be documented in a separate, companion report.

Approach

The U.S. Army Engineer Research and Development Center (ERDC) conducted a series of high strain-rate tests on five types of mechanical couplers used for splicing flexural reinforcing steel. Each coupler system was tested at three strain rates. For each mechanical coupler and strain-rate combination, three specimens were tested to develop average properties defining the strength and ductility of the coupler system. A total of 45 tests were performed.

A 200,000-lb dynamic loader (Huff 1969) was used to apply the required load at slow, intermediate, and rapid strain rates. The strain rates achieved were between 0.001 and 3.5 sec^{-1}.

2   Test Description

Three series of experiments were conducted in this study. The first and second series consisted of basic reinforcement bar material property tests in which the bars were tested in both the "machined" and "as-rolled" condition. The third series of experiments consisted of testing the mechanical couplers installed on the reinforcing bars. All test specimens were pulled in the vertical position.

The experimental parameters for the first two series of experiments were the condition of the reinforcement bar (as-rolled or machined) and the dynamic load condition (strain rate). The experimental parameters for the third series of experiments were the type of mechanical coupler and dynamic load condition (strain rate). These parameters are discussed in the following sections.

Mechanical couplers

Coupler selection process

American Concrete Institute (ACI) standard 439.3R-07 (ACI 2007) was used as a guide for selecting five types of mechanical couplers. Table 2.1 of that standard provides a list of the types of mechanical couplers available in the market today. The couplers listed in the table are suitable for tension and compression applications for both type 1 and type 2 connections using ASTM A615 Grade 60 reinforcement bar under ACI standard 318-02 (ACI 2002). ACI 439.3R-07 states that the ACI 318 type 1 connections are used in elements where there is little concern for inelastic deformations and elevated tensile stresses from seismic events. ACI 318 type 2 connections have demonstrated, through accepted industry testing, the ability to develop the specified tensile strength of the spliced bars for resistance to elevated tensile stresses. Only ACI 318 type 2 mechanical connectors were selected for this series of tests.

Using Table 2.1 (ACI 2007) to further narrow the selection, couplers that were shown to provide versatility in the categories of application and suitability were selected. Four types of couplers were initially selected:

- Cold-swaged-steel coupling sleeve.

- Grout-filled coupling sleeve.
- Shear-screw and wedge coupling sleeve.
- Upset-bar and coupling sleeve with straight threads.

Other selection criteria were based on the ease of use and the selection of distinctly different couplers to provide a good cross section of applications and installation processes. The upset-bar type was selected over the cold-swaged type after review of its application in another government containment facility, and the specific application warrants further investigation. The sponsor selected and added a taper-threaded coupler system and a coupler system for thread-like deformed reinforcement bars to the experiment series. The final couplers selected for this series of experiments were the following:

- Upset-bar and coupling sleeve with straight threads.
- Grout-filled coupling sleeve.
- Shear-screw coupling sleeve.
- Taper-threaded system.
- Thread-like deformed reinforcement bar coupler system.

Mechanical coupler systems

The criteria for selection of the couplers to be tested consisted of the coupler's prior approval for seismic use and its ease of installation. The types selected for this study are generally categorized as "taper-thread," "upset," "grouted," "shear screw," and "rebar thread." These systems provide a good representation of the types of couplers commonly available and in use today.

Illustrated in Figure 3 (from left to right) and described below are the five couplers:

- Taper-threaded system: consists of tapered threads on each end of the rebar along with a male/female threaded coupler to form the connection between the two ends of the rebar.
- Upset-head system: an "upset" system that uses a formed head on each end of the rebar along with a male/female threaded coupler.
- Grouted-sleeve system: uses a sleeve in which the two ends of the rebar are "grouted" into the sleeve to make the connection.

Taper Thread	Upset Head	Grouted Sleeve	Shear Screw	Threaded Bar
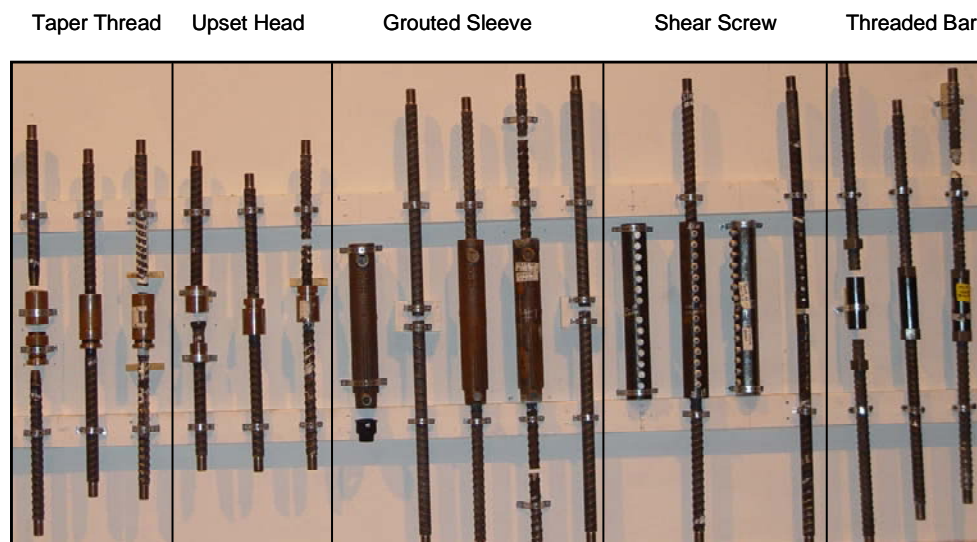
Figure 3. Mechanical couplers systems included in the test series.

- Shear-screw system: consists of a wedge-shaped coupling sleeve and "shear screws" to form the connection between the two ends of the rebar.
- Threaded-rebar system: consists of rebar with rolled-on deformations with a similar thread profile to that of a stub-acme thread. The coupler sleeve has matching internal threads and is locked in place with two similar threaded nuts at each end.

"Machine shop" and assembly drawings of these coupler systems are presented in Appendix A.

Concrete reinforcement bars

ASTM A615 Grade 60, Number 10, deformed reinforcement bars were tested at full size (as-rolled) to determine the ultimate dynamic load strength of the bar. The reinforcing bars were also machined to a standard "dog bone" shape and tested to determine the ultimate dynamic tensile strength of the bar for comparison with the static tensile strength from mill certifications and material test reports provided by the reinforcement bar manufacturer. Figure 4 shows the machined specimens in the left photo and the as-rolled reinforcement specimens in the photo to the right. Both are shown with their respective grip systems. All Grade 60 reinforcement bar tested was from the same lot and manufacturer. "Machine shop" drawings of the as-rolled and machined test specimens are presented in Appendix A.
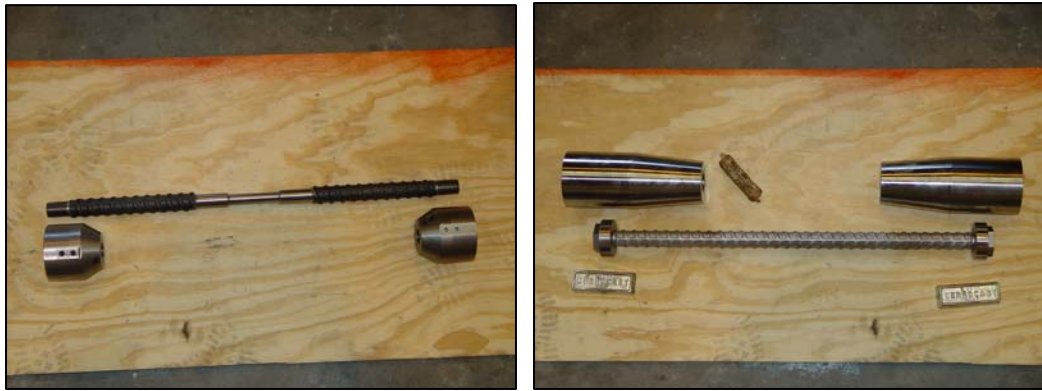
Figure 4. Machined (left) and as-rolled (right) reinforcement bars.

ASTM A615 Grade 75, Number 10, threaded deformed reinforcement bars were also tested at full size (as-rolled) to determine the ultimate dynamic load strength of the bar. All Grade 75 reinforcement bar tested was from the same lot and manufacturer. The ASTM A615 Grade 75 machined specimens were not tested in this series of experiments.

Experiment setup

Test matrix

Five types of mechanical couplers were tested in this test series and were identified as MC-1 through MC-5. Each coupler was subjected to three strain rates, and three couplers were tested for each type of coupler at each strain rate. The experiment matrix was designed based on prior experiments performed by William J. Flathau (Flathau 1971). The coupler test matrix is provided as Table 1.

Table 1. Mechanical coupler experiment matrix.

Coupler Identifier	Coupler Type	Number of Slow-Rate Tests	Number of Intermediate-Rate Tests	Number of Rapid-Rate Tests
MC-1	Upset	3	3	3
MC-2	Grouted	3	3	3
MC-3	Screwed	3	3	3
MC-4	Taper thread	3	3	3
MC-5	Threaded rebar	3	3	3

The ASTM A615 Grade 60 reinforcement bars were tested in two conditions, i.e., as-rolled and machined. The ASTM A615 Grade 75

reinforcement bars were tested only in the as-rolled condition. Each condition of the reinforcement bar was subjected to three strain rates. The reinforcement bar test matrix is provided as Table 2.

Table 2. Reinforcement bar experiment matrix.

Reinforcement Bar	Reinforcement Bar Condition	Number of Slow-Rate Tests	Number of Intermediate-Rate Tests	Number of Rapid-Rate Tests
RB-1 (Grade 60)	As-rolled, deformed	3	3	3
RB-3 (Grade 60)	Machined, deformed	3	3	3
RB-4 (Grade 75)	As–rolled, threaded deformed	3	3	3

200,000-lb dynamic loader

The dynamic loader (Figures 5 and 6) is a device capable of applying a concentrated load in short times over a maximum stroke of 6 in. This loader has the capability to test structural shapes with loading rates varying from slow static loads to those at which the maximum load is reached in very few milliseconds. The applied loads can be varied from 10,000 to 200,000 lb in either tension or compression. The design of the device is such that loads as high as 400,000 lb may be possible; however, the maximum load capacity of the device is dependent on the use to which it is subjected.

The maximum time required to develop a specific load is affected by many variables, including piston location, magnitude of load, response of resisting test specimen, and characteristics of the control valves, etc. Therefore, the rise-time characteristics of the loader are a function of the test condition. A minimum rise time of 1.3 msec for a load in excess of 200,000 lb with approximately 1/4-in. movement of the piston has been obtained with the device.

For the tests documented herein, the loader was configured to allow slow, intermediate, and rapid strain rates as required by the sponsor. These
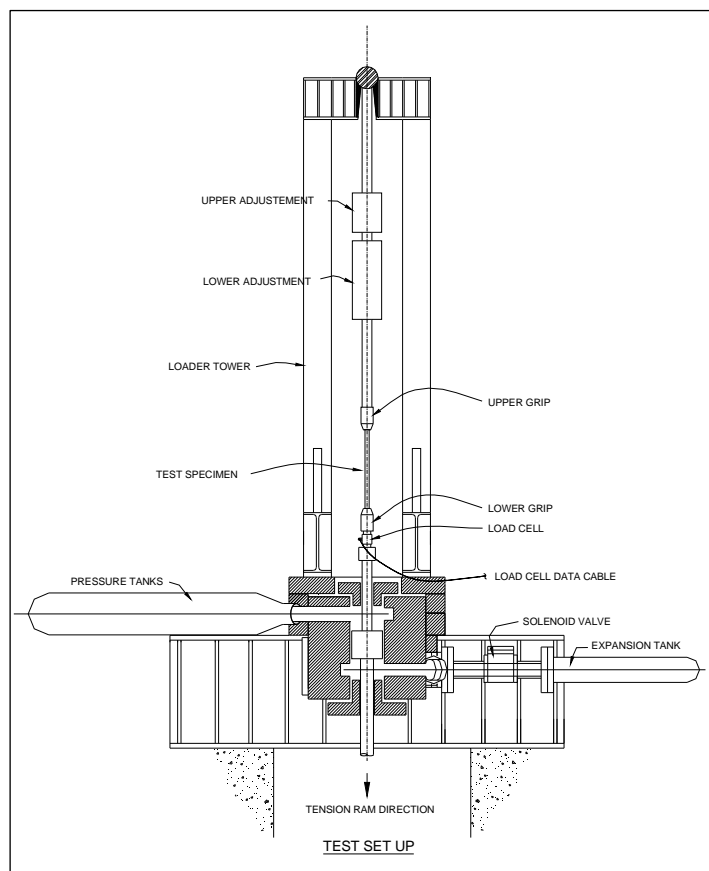
Figure 5. Schematic of 200,000-lb hydraulic dynamic loader.

strain rates ranged from 0.001 sec^{-1} to 3.5 sec^{-1}. The loader was calibrated by pulling several machined rebar specimens at each expected strain rate.

Rapidly applied loads may have an inertial force component that should be accounted for when determining the actual applied load on the specimen. This inertial force is due to the acceleration of the large masses associated with the loading system. The rapid strain-rate experiments required load corrections due to the inertial effects of the acceleration of the mass of the reinforcement bar, the mechanical coupler, and the gripping system of the loader.

Figure 7 shows the significant correction to the load at the rapid rate of strain. The correction is easily applied using a data plotting program to add the uncorrected curve (shown in black in Figure 7) to the inertia correction load (shown in red). This correction provides the final load curve (shown in green), which represents the actual applied load on the test specimen.
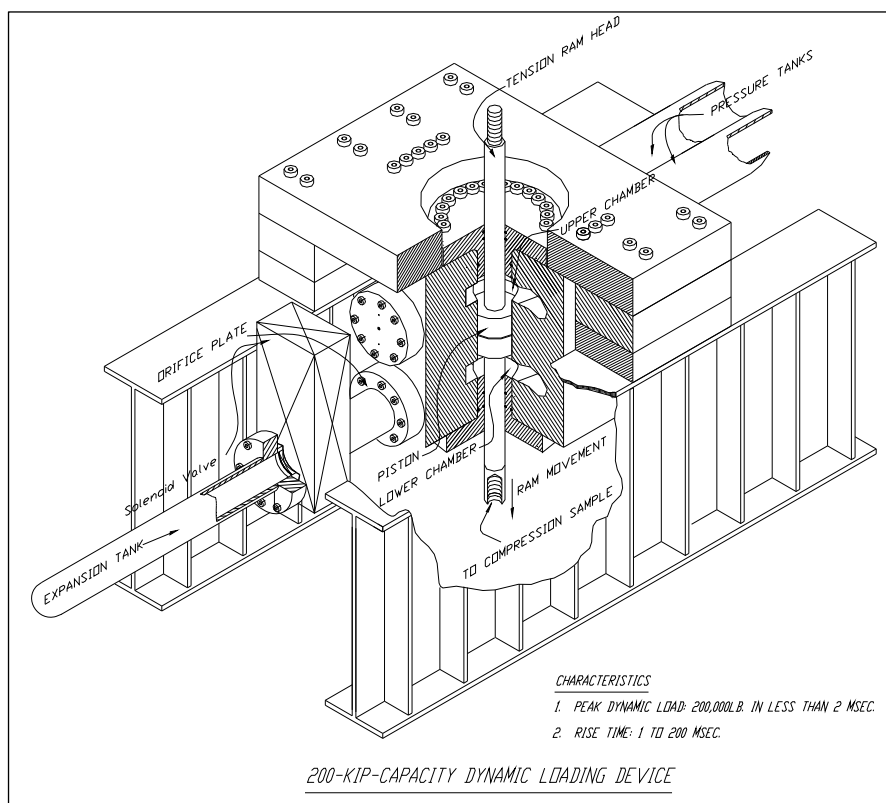
Figure 6. Three-dimensional view of 200,000-lb loader.
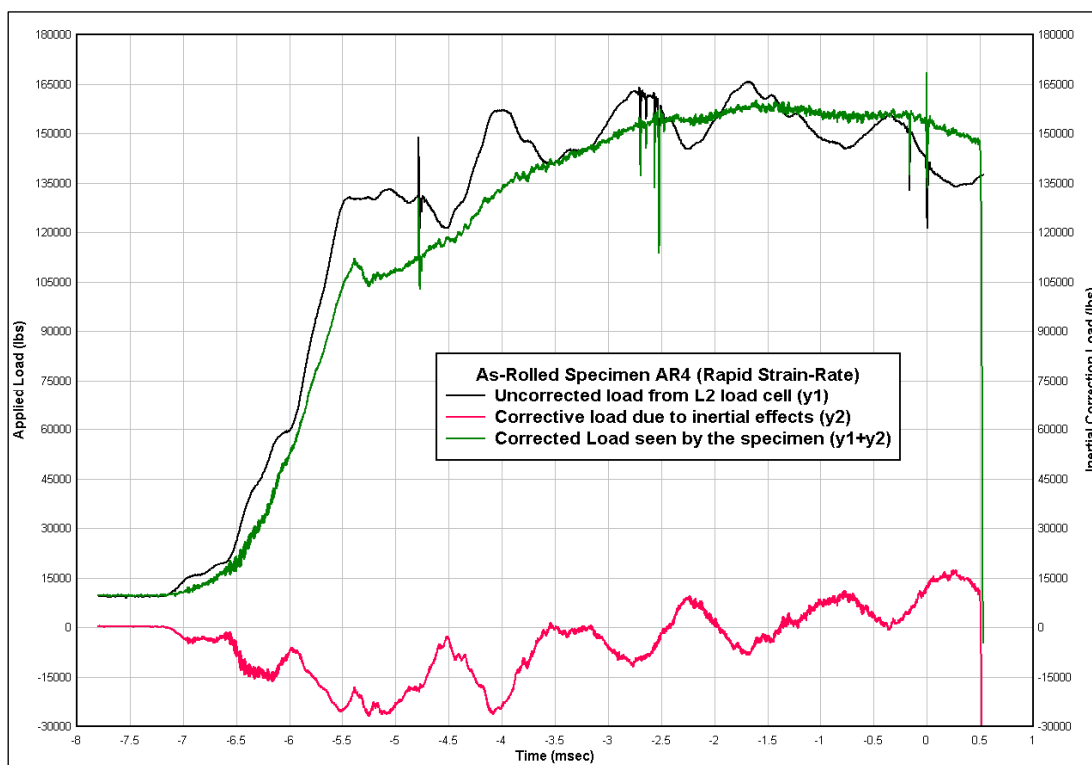
Figure 7. Example of correction on applied load due to inertial effects during
rapid-strain rate tests.

Instrumentation

Acceleration, coupler and rebar strain, applied load, and load duration
were recorded during each test. An accelerometer was hard-mounted to
both the upper and lower loader grips for the purpose of recording
acceleration time-histories. Four strain gages were installed on the
reinforcing bar to record longitudinal rebar strains on each side of the bar.
Up to four strain gages, depending on the type of coupler being tested,
were installed on each mechanical coupler to record longitudinal coupler
strains. Two load cells, one upper and one lower, were used to record the
reactive and applied loads, respectively.

Load cells

The load cells were made from 4130 quench and tempered steel with a
minimum yield strength of 100,000 psi and a maximum capacity of
greater than 200,000 lb. The load cells were capable of measuring both
the applied and reaction forces during the test. The load cells were
attached to the loader grips at each end of the test specimen, and then to
the loader tower at the top end and to the loader ram at the bottom end.
Four strain gages were attached 90 deg apart to measure the longitudinal
and circumferential strains. These gages were connected electronically to
form a Wheatstone bridge. This configuration allowed the net contribution
to remain positive whether the load is in tension or compression. Each
load cell was calibrated before the test series.

Strain gages

Reinforcing-bar strains were measured using Model CEA-06-062-350-UW
1/16-in. strain gages from Measurements Group. Four strain gages were
mounted in the longitudinal direction between the bar deformations as
close to 90 deg apart as possible. (See location SG1 in top view of Fig-
ures A1–A6,) For the tensile strength property on the machined bar, three
sets of gages (SG3, SG2, and SG4) were mounted, as shown in the bottom
view of Figure A1.

Coupler strains were measured using similar 1/4-in. strain gages placed on
the outside of the couplers 180 deg apart. The upset-head, taper-threaded,
and threaded-bar couplers had two gages placed along the length of the
coupler at the thinnest part of the coupler wall (location SG2 in Fig-
ures A2, A5, and A6). The shear screw had two sets (locations SG2 and

SG3 in Figure A4) and the grouted couplers had three sets (locations SG2, SG3, and SG4 in Figure A3) of two gages mounted in the longitudinal direction 180 deg apart on the outside of the coupler equally spaced from the ends of the coupler.

Accelerometers

Endevco Model 7270A accelerometers were used to determine the acceleration time-histories of the mass of the grips at the end of the bar for monitoring inertial effects. The accelerometers were hard-mounted to 1-in. steel blocks that were in turn mounted to the sides of the upper and lower grips.

High-speed photography

A high-speed, 10,000-fps digital camera was used to record the tests and capture the displacement histories at multiple locations, allowing the computation of strain on the test specimens past the capacity of the strain gages. A regular digital/video camera was used to record an overall view of selected experiments during the test series. Still photographs and video were also obtained during the construction, test preparation, test execution, and posttest disassembly.

3   Test Results

Comparison of the performance of the control specimen and performance of the selected mechanical couplers must be made to determine if the criteria given in Section 4-21.8 of TM 5-1300 (Department of Army 1990) was achieved. This criteria states that devices for mechanical splices of reinforcement may be used for end anchorage and splices in reinforcement if they are capable of developing the ultimate dynamic tensile strength of the reinforcement without reducing its ductility.

To determine the adequacy of these devices, a control specimen was first tested to determine the dynamic material properties of the reinforcement material at the desired strain rate under which the selected couplers would be subjected. The coupler systems were then tested at the same strain rate and in the same manner in which the control specimen was tested. The data collected from the results of each of the two test series were then compared.

Several failures occurred in the rebar at the location of the strain gages. It is possible that failure occurred at this location because a minute amount of material had been removed from the bar to provide a clean and smooth bonding surface for the strain gages. It is also possible that this affected the ultimate dynamic strengths of the specimens. However, the overall results are considered to be valid because both the control specimens and the coupler specimens were prepared for strain gages in the same location, manner, and procedure.

As-rolled control specimens

Two types of as-rolled (AR) reinforcement bars were tested. The first type of reinforcement bar was ASTM 615 Grade 60. This type was used in all tests except for the threaded rebar system (MC-5 and RB-4) series of tests. The second type was ASTM 615 Grade 75. Testing of the second type was required because the MC-5 coupler system required a special threaded rebar that was available only in Grade 75. Figures 8–10 show the test results of the ASTM 615 Grade 60 tests at the slow, intermediate, and rapid strain rates, respectively.

Figure 8. Stress vs. strain for AR ASTM 615 Grade 60 steel slow-strain rate specimens.

Figure 9. Stress vs. strain for AR ASTM 615 Grade 60 steel intermediate-strain rate specimens.

Figure 10. Stress vs. strain for AR ASTM 615 Grade 60 steel rapid-strain rate specimens.

The stress and strain values at the yield point were recorded as the yield stress and yield strain, respectively, for all ASTM 615 Grade 60 control bars tested at the rapid strain rate. These values were compared to the stresses and strains at the yield point for all ASTM 615 Grade 60 coupler systems tested at the rapid strain rate. The slow and intermediate strain-rate tests used the 0.2% offset method to determine the yield stress and yield strain. These values were compared to the results of the ASTM 615 Grade 60 coupler systems tested at the slow and intermediate strain rates.

Table 3 shows the test results from each of the as-rolled ASTM 615 Grade 60 reinforcement bars pulled at the three strain rates. Also shown in the table are the average values of yield stress, strain at yield, dynamic ultimate strength, maximum strain (strain at rupture), ductility ratio (strain at rupture divided by strain at yield), percent elongation, and strain rate.

Figures 11–13 show the test results of the as-rolled threaded reinforcement bar (ART), ASTM 615 Grade 75 steel tests at the slow, intermediate, and rapid strain rates.

Table 3. Test results from AR ASTM 615 Grade 60 reinforcement bar control specimens.

Specimen Name	Specimen Number	Yield Stress (psi)	Yield Strain (µin./in.)	Dynamic Ultimate Strength (psi)	Maximum Strain (µin./in.)	Ductility Ratio	Elongation %	Strain Rate (in./in./sec)
AR6	RB-1-6	69,800	5,100	118,100	105,100	20.7	10.5	0.0035
AR11	RB-1-11	71,900	5,400	116,700	92,800	17.1	9.3	0.0039
AR12	RB-1-12	70,600	5,100	117,000	104,300	20.3	10.4	0.00037
AR-Slow	**Average**	**70,800**	**5,200**	**117,000**	**100,800**	**19.4**	**10.1**	**0.0037**
AR5	RB-1-5	72,600	5,200	119,800	118,000	22.7	11.8	0.060
AR9	RB-1-9	-----	-----	-----	----	-----	----	-----
AR10	RB-1-10	77,000	5,400	119,200	92,000	17.0	9.2	0.068
AR-Inter	**Average**	**74,800**	**5,300**	**119,500**	**105,000**	**19.9**	**10.5**	**0.064**
AR4	RB-1-4	90,400	4,100	129,500	149,000	36.3	14.9	3.3
AR7	RB-1-7	89,000	5,400	130,700	144,000	26.7	14.4	3.2
AR8	RB-1-8	90,000	4,700	128,700	120,000	25.5	12.0	3.1
AR-Rapid	**Average**	**89,800**	**4,700**	**129,600**	**138,000**	**29.5**	**13.8**	**3.2**
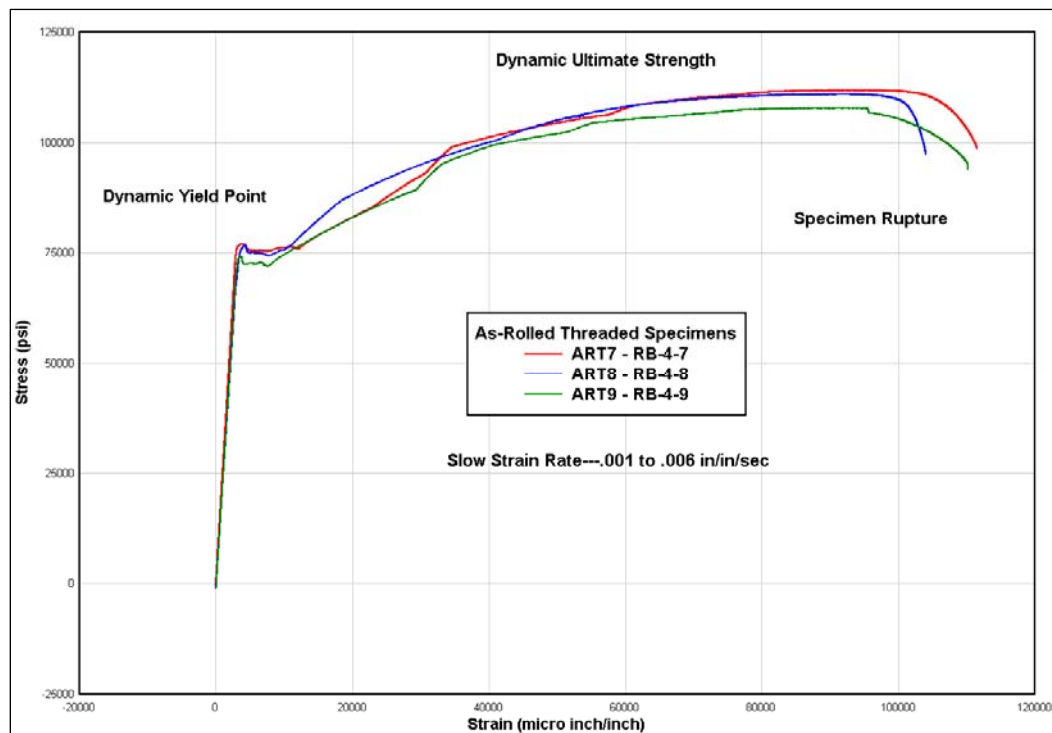
Figure 11. Stress vs. strain for ART ASTM 615 Grade 75 steel slow-strain rate specimens.
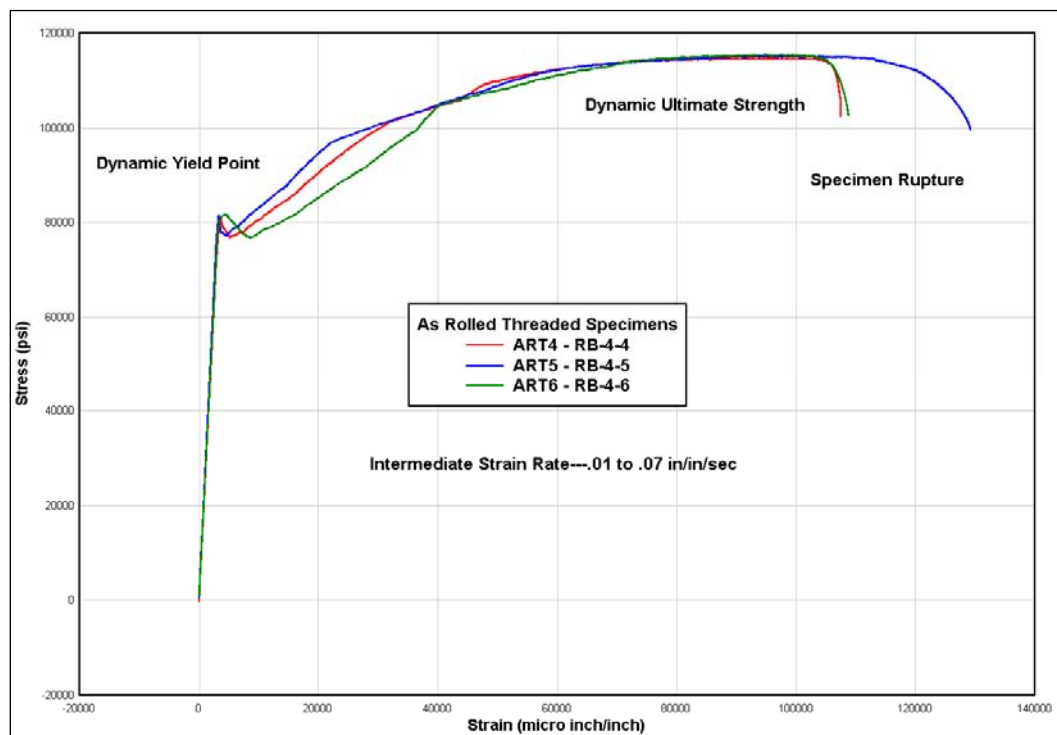
Figure 12. Stress vs. strain for ART ASTM 615 Grade 75 steel intermediate-strain rate specimens.
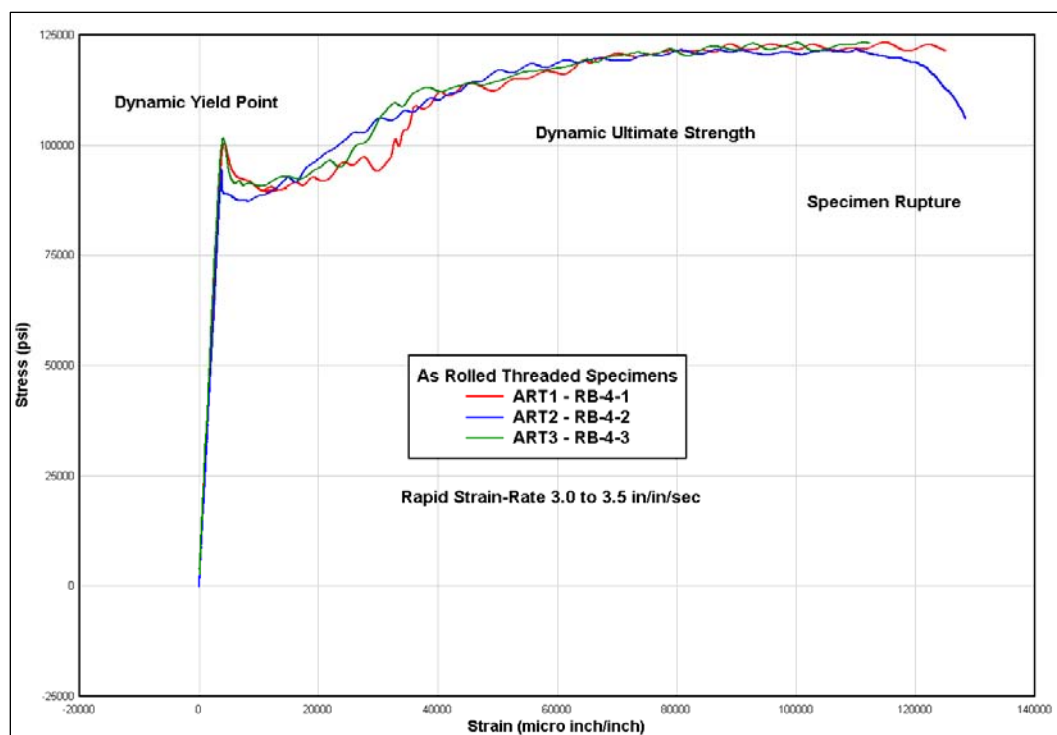
Figure 13. Stress vs. strain for ART ASTM 615 Grade 75 rapid-strain rate specimens.

The stress and strain values at the yield point were again recorded as the yield stress and yield strain, respectively, for all ASTM 615 Grade 75 control bars. These values were compared to the results of the ASTM 615 Grade 75 coupler systems.

Table 4 shows the test results from each of the as-rolled ASTM 615 Grade 75 reinforcement bars pulled at the three strain rates. Also shown in the table are the values for each measurement set.

Table 4. Test results from ART ASTM 615 Grade 75 reinforcement bar control specimens.

Specimen Name	Specimen Number	Yield Point Stress (psi)	Yield Point Strain (μin./in.)	Dynamic Ultimate Strength (psi)	Maximum Strain (μin./in.)	Ductility Ratio	Elongation %	Strain Rate (in./in./sec)
ART7	RB-4-7	77,100	4,000	112,100	111,500	28.0	11.2	0.0030
ART8	RB-4-8	76,900	4,300	111,100	104,000	24.5	10.4	0.0033
ART9	RB-4-9	74,300	3,700	108,000	110,200	30.0	11.0	0.0031
ART-Slow	Average	76,100	4,000	110,400	108,600	27.5	10.9	0.031
ART4	RB-4-4	81,300	3,600	114,700	107,600	29.5	10.8	0.053
ART5	RB-4-5	81,600	3,300	115,200	129,100	38.9	12.9	0.051
ART6	RB-4-6	81,700	4,400	115,600	108,800	24.6	10.9	0.053
ART-Inter	Average	81,500	3,800	115,200	115,200	31.0	11.5	0.052
ART1	RB-4-1	100,600	4,300	123,400	125,000	29.1	12.5	3.3
ART2	RB-4-2	94,700	3,800	121,700	128,400	33.6	12.8	3.0
ART3	RB-4-3	101,600	4,000	123,300	112,400	27.8	11.2	3.4
ART-Rapid	Average	99,000	4,000	122,800	122,000	30.2	12.2	3.2

Machined reinforcement bar

Nine specimens of the ASTM 615 Grade 60 bars (see lower drawing in Figure A1) were machined to 0.75-in. diameter at the midsection to ensure failure within the 3-in. gage length for the purpose of determining dynamic material properties. These machined bars (MB) were tested at the three strain rates. The ASTM 615 Grade 75 bars were not tested in the machined condition. Figures 14–16 show the test results of the ASTM 615 Grade 60 tests on machined bars at the slow, intermediate, and rapid strain rates.
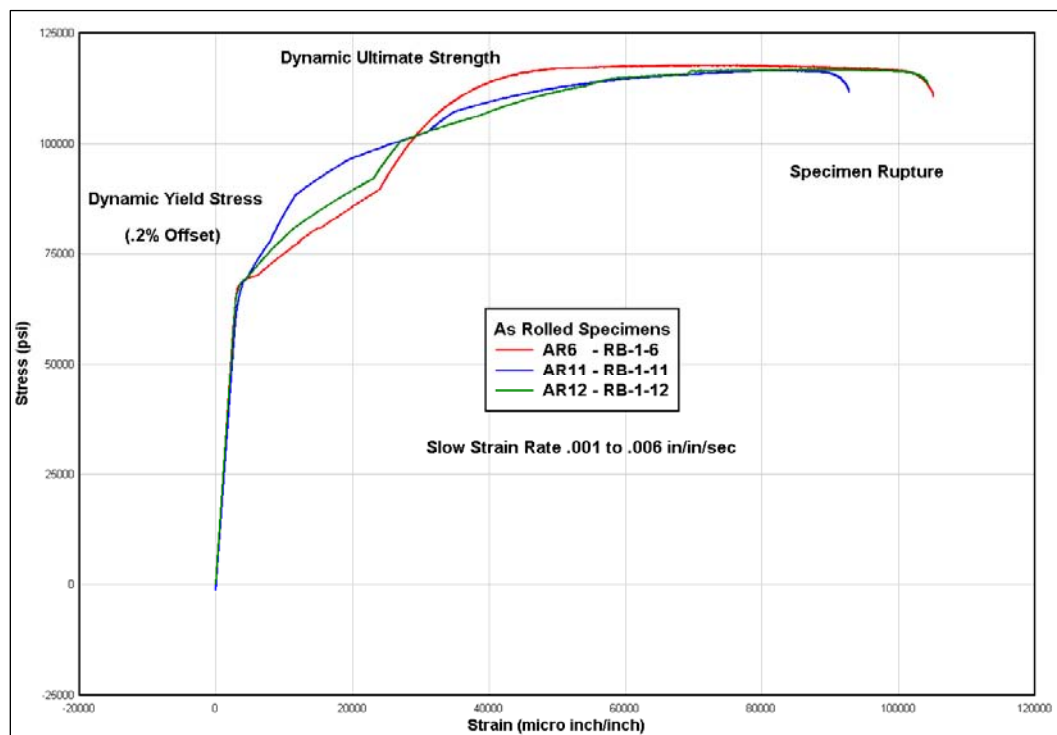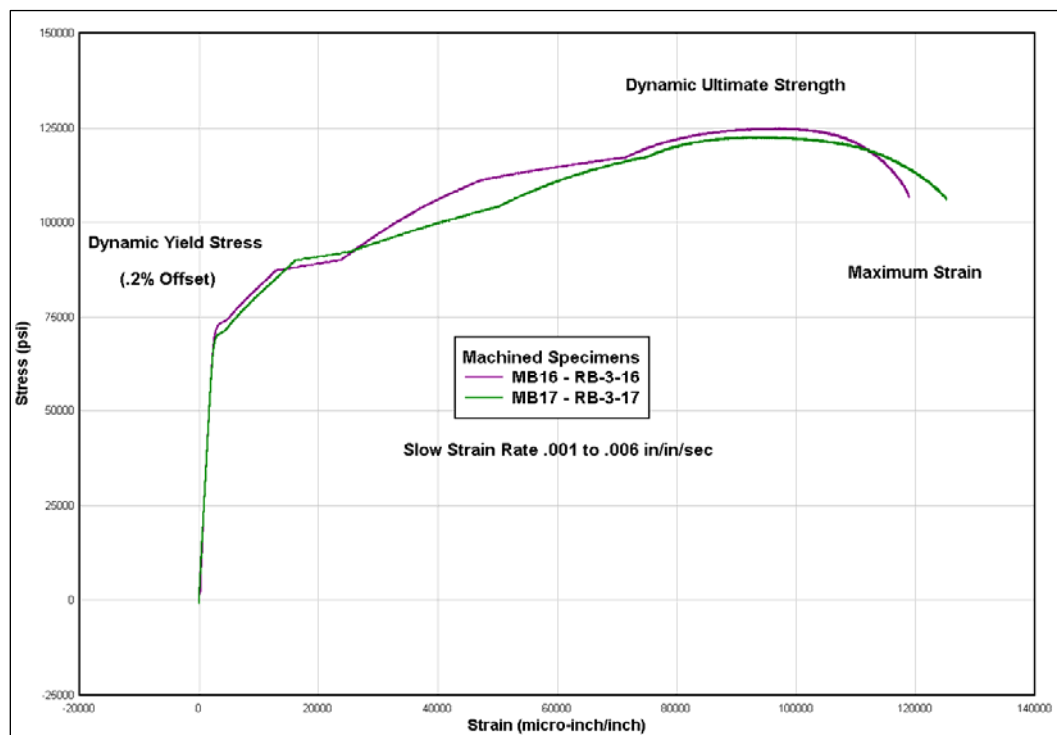
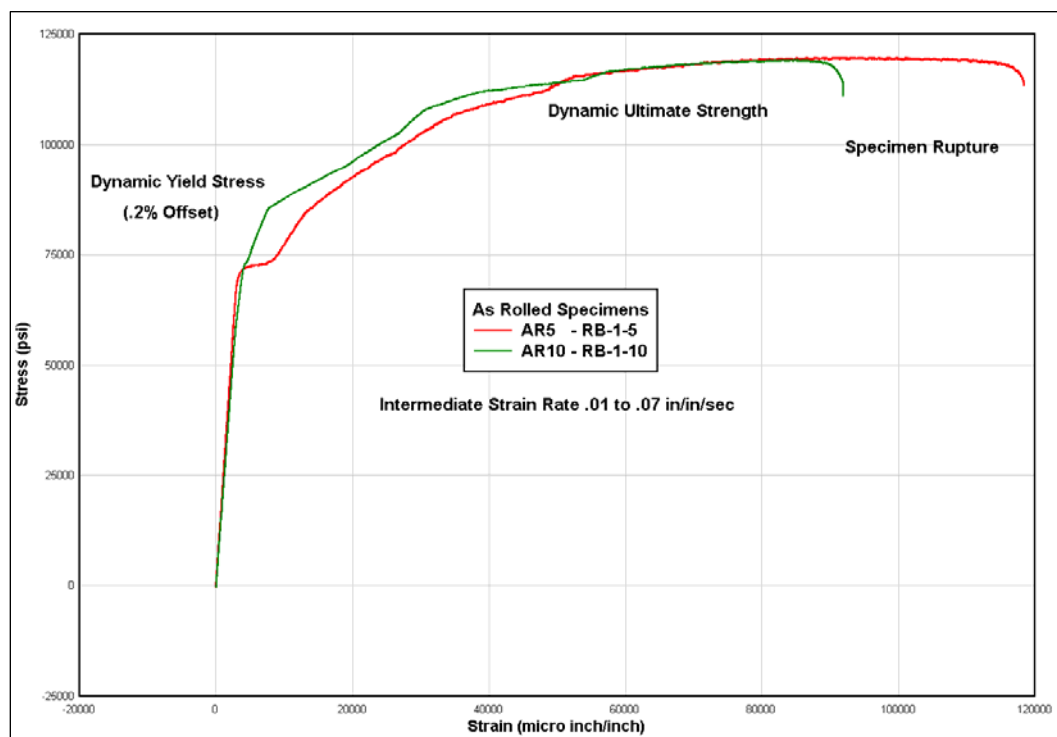Figure 14. Stress vs. strain for MB ASTM 615 Grade 60 steel slow-strain rate specimens.

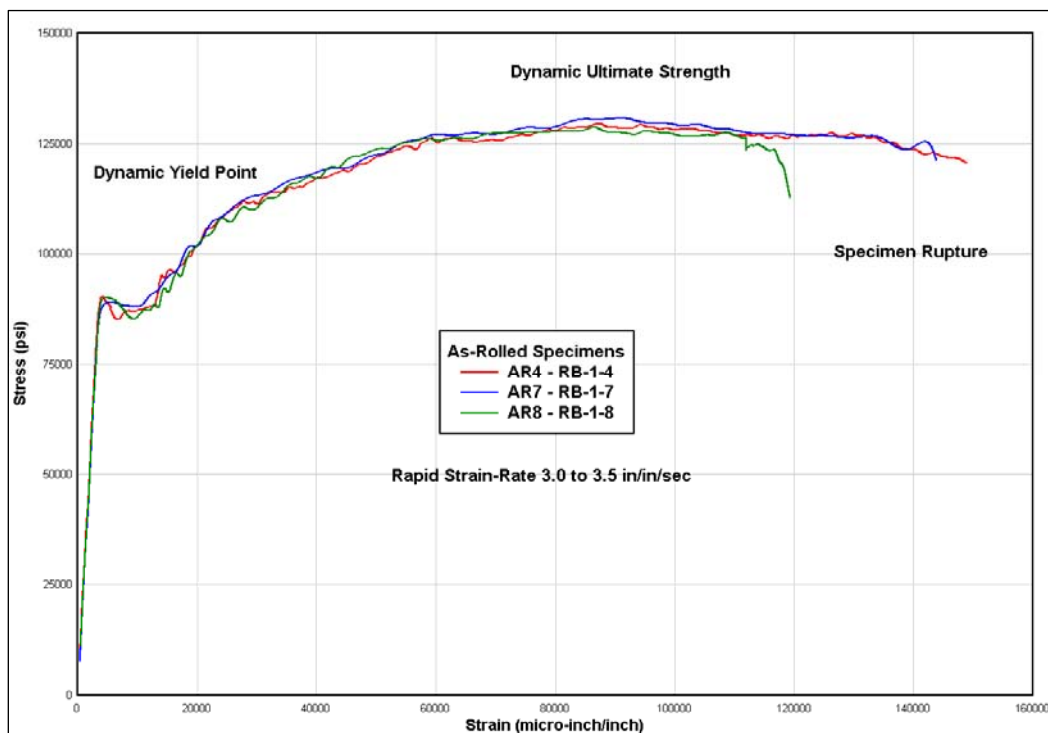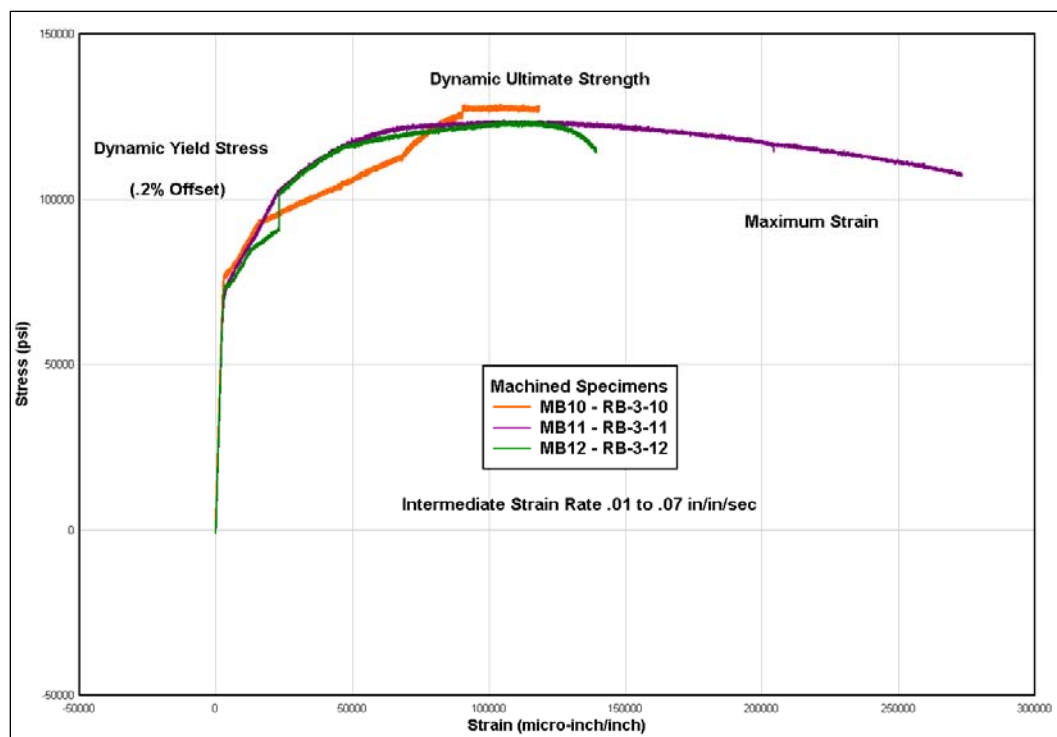Figure 15. Stress vs. strain for MB ASTM 615 Grade 60 steel intermediate-strain rate specimens.
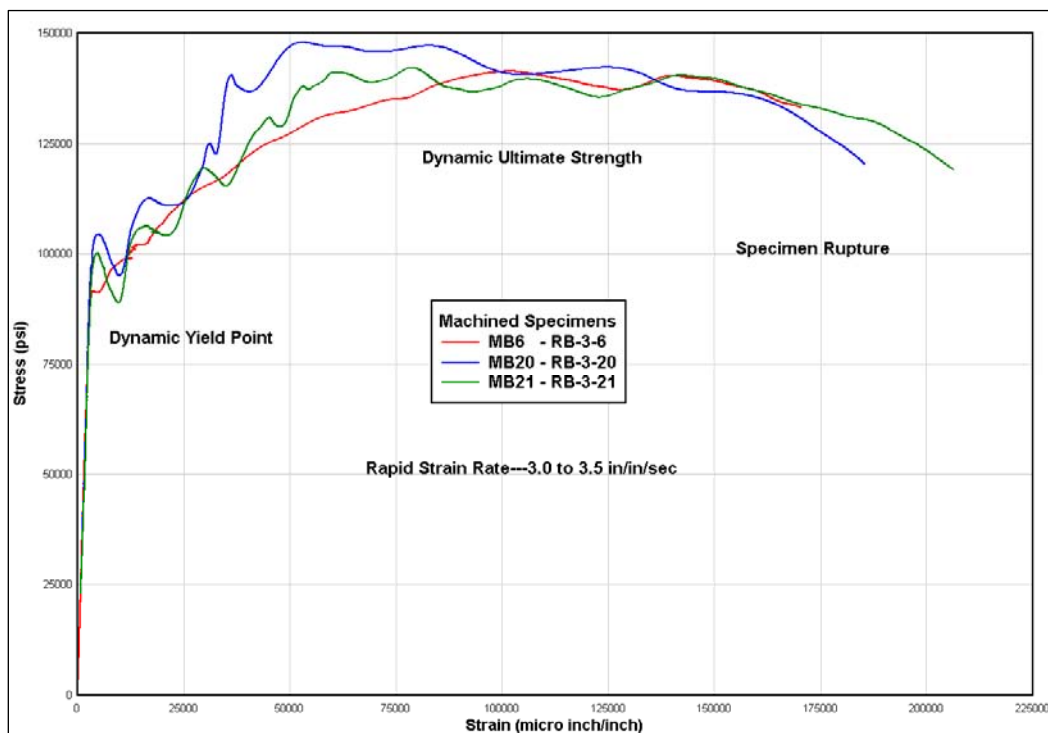
Figure 16. Stress vs. strain for MB ASTM 615 Grade 60 steel slow-strain rate specimens.

The stress and strain at the yield point were recorded as the yield stress and yield strain, respectively, for all ASTM 615 Grade 60 machined bars tested at the rapid strain rate. The slow and intermediate strain-rate tests again used the 0.2% offset method to determine the yield stress and strain at yield.

Table 5 shows the test results from each of the MB ASTM 615 Grade 60 reinforcement bars pulled at the three strain rates. Also shown in the table are the average values for each measurement set.

Upset head system

Slow strain rate

Failure occurred in all three specimens in the rebar outside the heat-affected zone. No data were collected in the plastic strain region for specimen UHC9 because of a malfunction of the high-speed video data. Specimens UHC10 and UHC11 developed a dynamic ultimate tensile strength greater than that of the control bar and surpassed the ductility of the control bar. The breaks in the bars to the right of the couplers (shown in the right photo of Figure 17) are the actual location of the bar failure.

Table 5. Test result from MB ASTM 615 Grade 60 steel reinforcement bar specimens.

Specimen Name	Specimen Number	Yield Stress (psi)	Yield Strain (µin./in.)	Dynamic Ultimate Strength (psi)	Maximum Strain (µin./in.)	Ductility Ratio	Elongation %	Strain Rate (in./in./sec)
MB14	RB-3-14	-----	-----	-----	-----	-----	-----	-----
MB16	RB-3-16	74,300	4,600	125,000	118,900	25.8	11.8	0.002
MB17	RB-3-17	71,500	4,500	122,700	125,200	27.7	12.5	0.002
MB-Slow	**Average**	**72,900**	**4,550**	**123,900**	**122,000**	**26.8**	**12.2**	**0.002**
MB10	RB-3-10	74,100	4,800	128,900	118,600	24.8	11.8	0.059
MB11	RB-3-11	75,300	4,800	124,100	273,400	56.6	27.3	0.072
MB12	RB-3-12	78,100	4,900	123,800	139,400	28.2	13.9	0.071
MB-Inter	**Average**	**75,800**	**4,800**	**125,600**	**177,100**	**36.5**	**17.7**	**0.067**
MB6	RB-3-6	91,600	3,700	141,400	170,300	46.2	17.0	3.56
MB20	RB-3-20	104,400	4,800	147,900	185,400	38.8	18.5	3.60
MB21	RB-3-21	100,300	4,600	142,200	206,400	45.1	20.6	3.31
MB-Rapid	**Average**	**98,800**	**4,400**	**143,800**	**187,400**	**43.4**	**18.7**	**3.49**
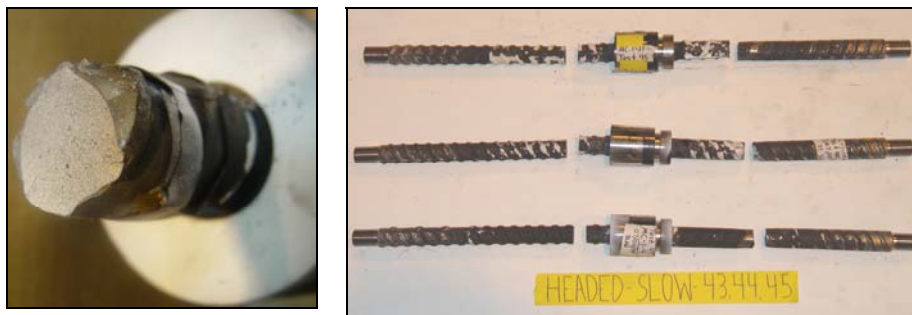
Figure 17. Posttest photos of upset head specimens tested at slow strain rate.

The breaks to the left of the couplers are where the bar was cut with a metal saw to allow for removal of the loader grip. The left photo in Figure 17 shows a typical tensile break.

Figure 18 shows the stress-strain test results from the coupler specimens tested at the slow strain rate. Table 6 compares the test results of each of the upset head coupler specimens to the average test results of the ASTM 615 Grade 60 control bars pulled at the slow strain rate. Also shown in the table are the average values for each measurement set.

Figure 18. Stress vs. strain for upset head coupler system at the slow strain rate.

Table 6. Test results of upset head coupler system at slow strain rates.

Specimen Name	Specimen Number	Yield Stress (psi)	Yield Strain (μin./in.)	Dynamic Ultimate Strength (psi)	Maximum Strain (μin./in.)	Ductility Ratio	Elongation %	Strain Rate (in./in./sec)
AR-Slow	Average	70,800	5,200	117,000	100,800	19.4	10.1	0.0037
UHC9	MC-1-9	-----	-----	-----	-----	-----	-----	-----
UHC10	MC-1-10	70,900	5,000	119,279	111,836	22.3	11.2	0.003
UHC11	MC-1-11	71,100	5,000	119,145	101,636	20.2	10.2	0.003
UHCA	Average	71,000	5,000	119,200	106,700	21.3	10.7	0.003

Intermediate strain rate

The three specimens failed in three failure modes. Specimen UHC6 (bottom right in Figure 19) failed in the rebar outside the heat-affected zone. This zone is an area extending from the flat face of the upset head, continuing along the length of the bar (approximately two diameters) that was subjected to the heating (2200 to 2500 °F) required to form the upset head shape. Specimen UHC7 (middle right in Figure 19) failed in the heat-affected zone in the rebar. Specimen UHC8 (top right in Figure 19) failed in the bar just below the upset head in the heat-affected zone.

Figure 19. Posttest photos of upset head specimens tested at intermediate strain rate.

Specimens UHC6 and UHC7 developed a dynamic ultimate tensile strength equal to or greater than that of the control bar but did not achieve the ductility of the control bar. Specimen UHC 9 failed close to the ulti-mate dynamic tensile strength of the control bar and also did not achieve the ductility of the control bar. The left photo in Figure 19 shows the fail-ure in the heat-affected zone just below the upset head. The breaks to the left of the couplers are where the bar was cut with a metal saw to allow for removal of the loader grip.

Figure 20 shows the stress-strain test results from the coupler specimens tested at the intermediate strain rate.
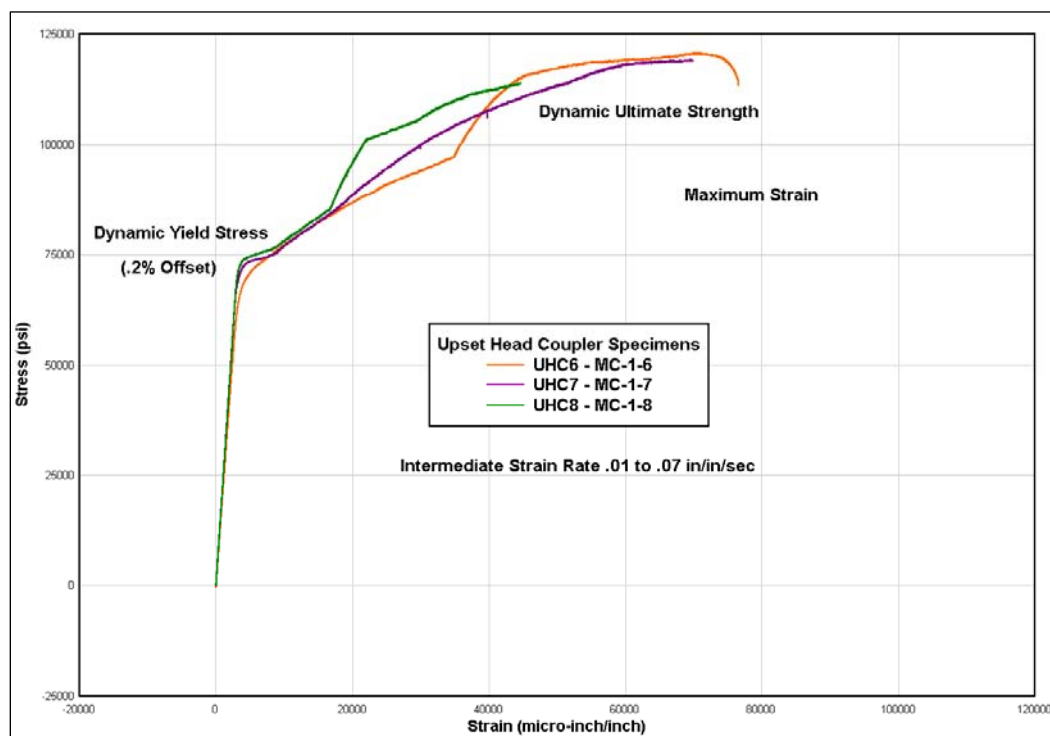
Figure 20. Stress vs. strain for upset head coupler system at the intermediate strain rate.

Table 7 compares the test results of each of the upset head coupler speci-
mens to the average test results of the ASTM 615 Grade 60 control bars
pulled at the intermediate strain rate. Also shown in the table are the val-
ues for each measurement set.

Table 7. Test results of upset head coupler system at intermediate strain rates.

Specimen Name	Specimen Number	Yield Stress (psi)	Yield Strain (μin/in)	Dynamic Ultimate Strength (psi)	Maximum Strain (μin/in)	Ductility Ratio	Elongation %	Strain Rate (in/in/sec)
AR-Inter	Average	74,800	5,300	119,500	105,000	19.9	10.5	0.064
UHC6	MC-1-6	71,700	5,500	120,900	76,600	14.0	7.6	0.068
UHC7	MC-1-7	73,600	5,200	119,300	69,900	13.5	6.9	0.059
UHC8	MC-1-8	74,800	5,200	114,000	44,700	8.6	4.4	0.058
UHCA	Average	73,400	5,300	118,100	63,700	12.0	6.3	0.062

Rapid strain rate

The specimens failed in three failure modes. Specimen UHC3 (bottom
right in Figure 21) failed in the rebar in the heat-affected zone. UHC5
(middle right in Figure 21) failed in the rebar outside the heat-affected
zone. UHC12 (top right in figure 21) failed just under the upset head in the
heat-affected zone. Specimens UHC3 and UHC12 failed to develop the
dynamic ultimate tensile strength or the required ductility. Specimen
UHC5 did achieve the dynamic ultimate tensile strength, came very close
to developing the required maximum strain, but did not achieve the
required ductility prior to failure. The left posttest photo in Figure 21
shows the failure that occurred inside the coupler just under the upset
head in the heat-affected zone.

Figure 21. Posttest photos of upset head specimens tested at rapid strain rate.

Figure 22 shows the stress-strain test results from the coupler specimens tested at the rapid strain rate. Table 8 compares the test results of each of the upset head coupler specimens to the average test results of the ASTM 615 Grade 60 control bars pulled at the rapid strain rate. Also shown in the table are the average values for each measurement set.
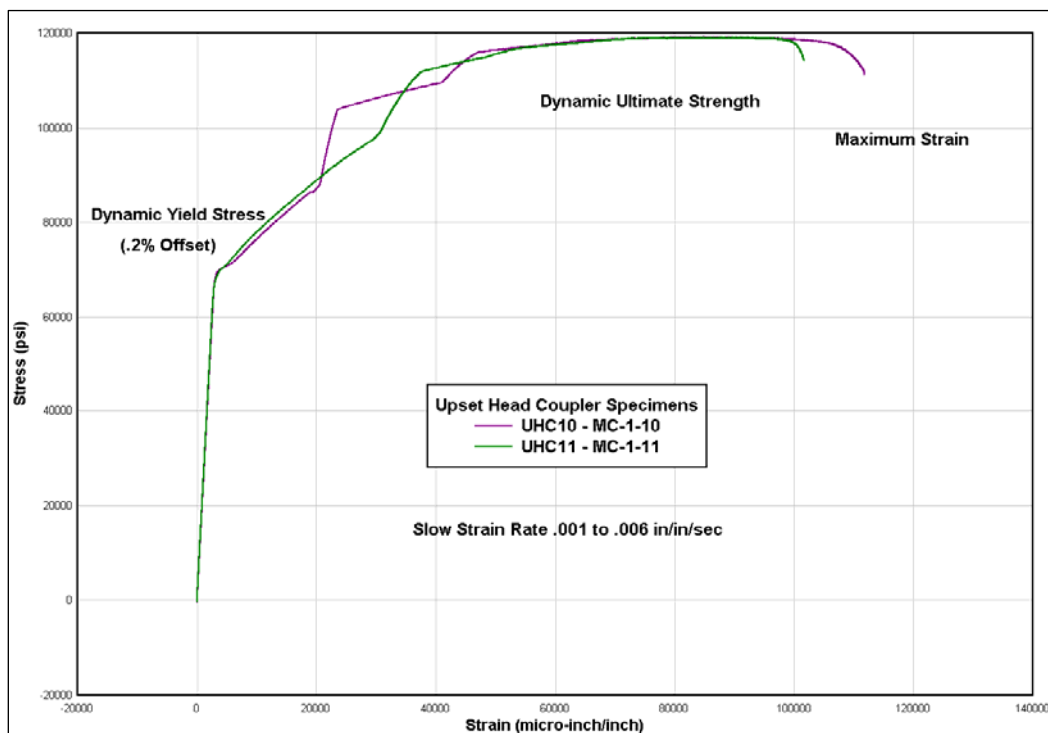

Figure 22. Stress vs. strain for upset head coupler system at the rapid strain rate.

Table 8. Test results of upset head coupler system at rapid strain rates.

Specimen Name	Specimen Number	Yield Stress (psi)	Yield Strain (µin./in.)	Dynamic Ultimate Strength (psi)	Maximum Strain (µin./in.)	Ductility Ratio	Elongation %	Strain Rate (in./in./sec)
AR-Rapid	Average	89,800	4,700	129,600	138,000	29.5	13.8	3.2
UHC3	MC-1-3	85,300	5,900	97,500	21,300	3.6	2.1	3.2
UHC5	MC-1-5	89,500	5,200	129,900	132,600	25.5	13.3	3.1
UHC12	MC-1-12	88,300	3,800	123,100	54,448	14.3	5.4	3.2
UHCA	Average	87,700	5,000	116,800	69,464	14.5	6.9	3.2

Grouted system

Slow strain rate

The three specimens failed in two failure modes. Specimen GSC7 (bottom right in Figure 23) failed because the rebar pulled out of the grout in the grout sleeve. The grouted sleeve was sliced longitudinally to reveal evidence of the rebar pullout (left photo in Figure 23). Specimens GSC8 and GSC9 (middle and top right, respectively, in Figure 23) failed at the midpoint of the cast steel grout sleeve. All three specimens almost developed the dynamic ultimate tensile strength of the control bar, but none achieved the ductility.

Figure 23. Posttest photos of grouted sleeve specimens tested at the slow strain rate.

Figure 23 shows the three specimens posttest and the grouted sleeve sliced longitudinally to reveal evidence of the rebar pullout.

Figure 24 shows the stress-strain test results from the coupler specimens tested at the slow strain rate.

Table 9 compares the test results of each of the grouted sleeve coupler specimens to the average test results of the ASTM 615 Grade 60 control bars pulled at the rapid strain rate. Also shown in the table are the average values for each measurement set.

Figure 24. Stress vs. strain for grouted coupler system at the slow strain rate.

Table 9. Test results of grouted coupler system at slow strain rates.

Specimen Name	Specimen Number	Yield Stress (psi)	Yield Strain (µin./in.)	Dynamic Ultimate Strength (psi)	Maximum Strain (µin./in.)	Ductility Ratio	Elongation %	Strain Rate (in./in./sec)
AR-Slow	Average	70,800	5,200	117,000	100,800	19.4	10.1	0.0037
GSC7	MC-2-7	71,000	5,300	115,800	65,800	12.5	6.6	0.004
GSC8	MC-2-8	70,400	5,000	114,000	67,400	11.6	5.7	0.003
GSC9	MC-2-9	69,200	5,200	113,900	60,000	11.6	6.0	0.004
GSCA	Average	70,200	5,100	114,500	61,100	11.9	6.1	0.004

Intermediate strain rate

The three specimens failed in two failure modes. Specimens GSC4 and GSC5 (bottom and middle right, respectively, in Figure 25) failed in the rebar outside the grouted sleeve. Specimen GSC6 (top right in Figure 25 failed at the midpoint of the cast steel grout sleeve. All three specimens developed the dynamic ultimate tensile strength of the control bar. However, none achieved the ductility of the control bar. The left photo in Figure 25 shows the grout sleeve coupler midpoint sleeve failure.

Figure 25. Posttest photos of grouted specimens tested at the intermediate strain rate.

Figure 26 shows the stress-strain test results from the coupler specimens tested at the intermediate strain rate.
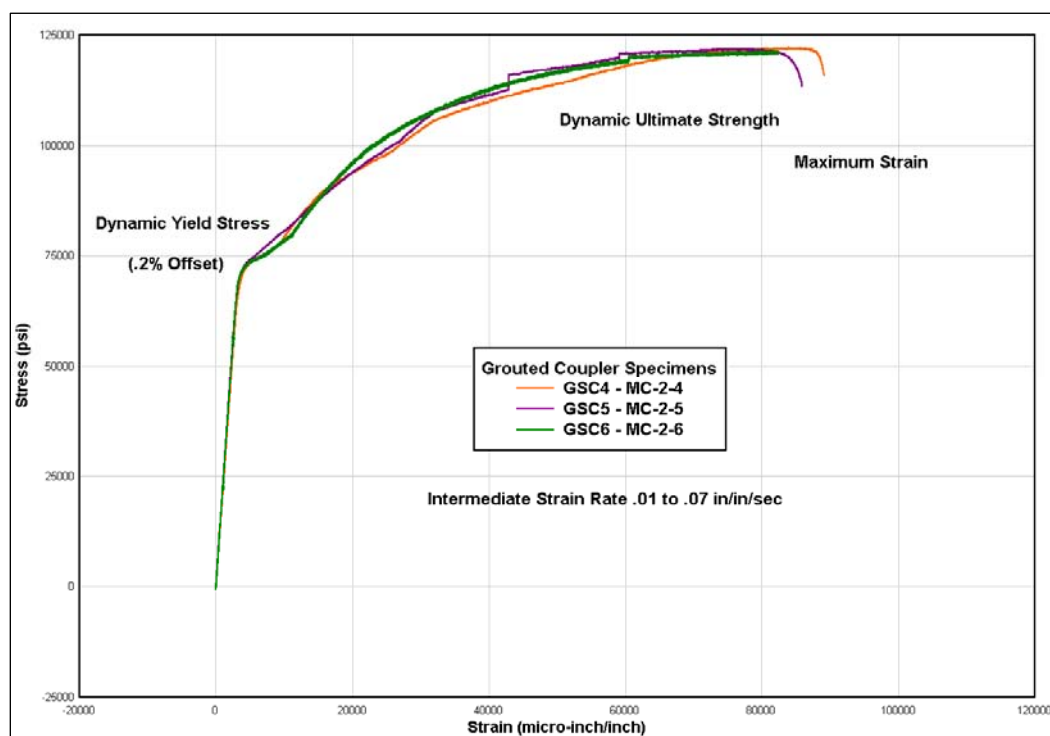
Figure 26. Stress vs. strain for grouted coupler system at the intermediate strain rate.

Table 10 compares the test results of each of the grouted coupler specimens to the average test results of the ASTM 615 Grade 60 control bars pulled at the intermediate strain rate. Also shown in the table are the average values for each measurement set.
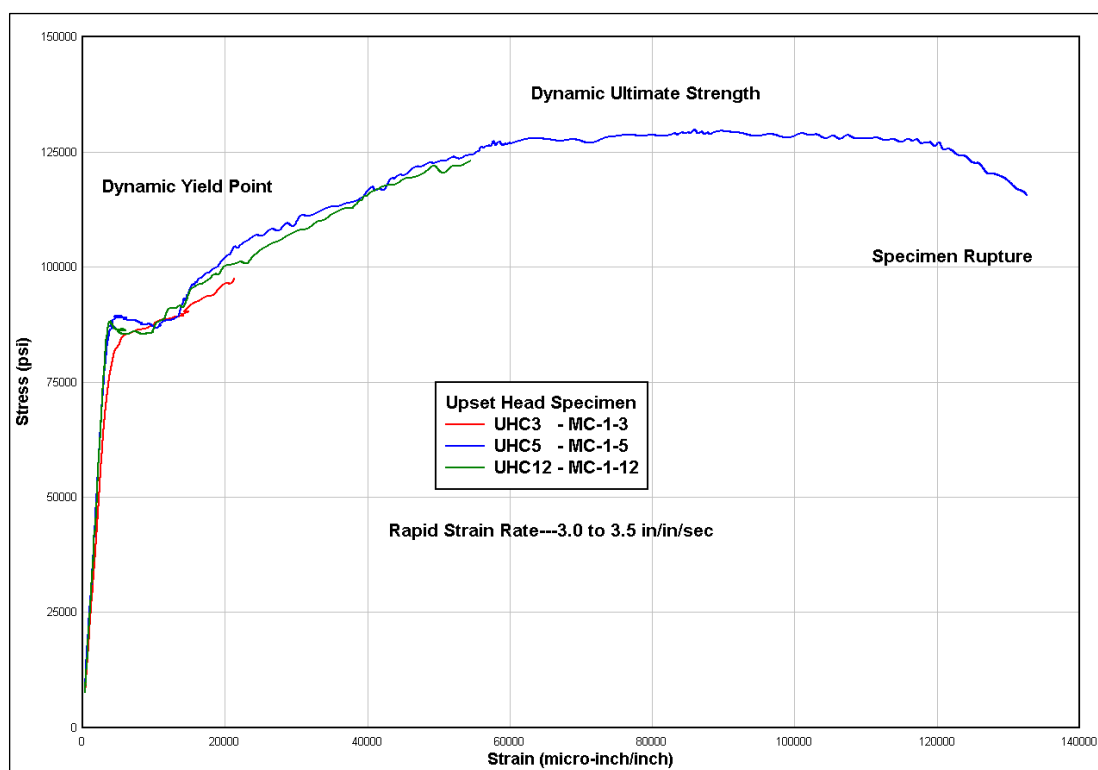
Table 10. Test results of grouted coupler system at intermediate strain rates.

Specimen Name	Specimen Number	Yield Stress (psi)	Yield Strain (μin./in.)	Dynamic Ultimate Strength (psi)	Maximum Strain (μin./in.)	Ductility Ratio	Elongation %	Strain Rate (in./in./sec)
AR-Inter	Average	74,800	5,300	119,500	105,000	19.9	10.5	0.064
GSC4	MC-2-4	73,900	5,500	122,300	89,100	16.1	8.9	0.063
GSC5	MC-2-5	74,700	5,400	122,100	85,900	16.0	8.6	0.059
GSC6	MC-2-6	74,000	5,300	121,600	82,400	15.4	8.2	0.060
GSCA	Average	74,200	5,400	122,000	85,800	15.8	8.6	0.061

Rapid strain rate

The specimens failed in three failure modes. Specimen GSC3 failed because of rebar pullout failure; specimen GSC2 failed because of sleeve failure; and specimen GSC1 failed because of rebar failure (bottom, middle, and top right, respectively, in Figure 27). Specimens GSC2 and GSC3 did not achieve the dynamic ultimate tensile strength or the required ductility of the control bar prior to failure. Specimen GSC1 did achieve the dynamic ultimate tensile strength but did not achieve the required ductility prior to failure. The left photo in Figure 27 shows the very violent midpoint sleeve failure.
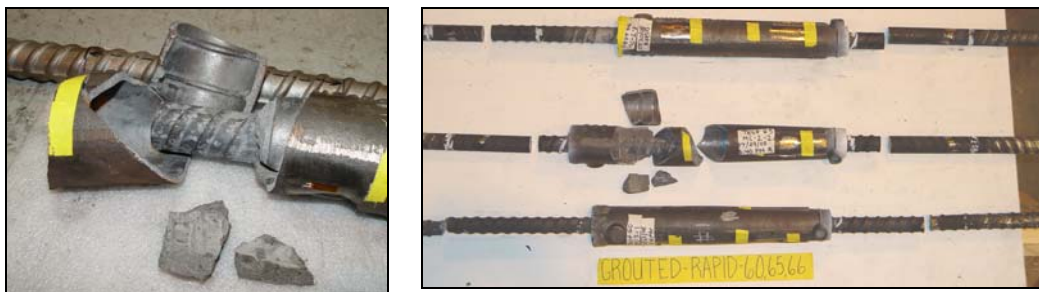
Figure 27. Posttest photos of grouted specimens tested at the rapid strain rate.

Figure 28 shows the stress-strain test results from the grouted sleeve coupler system tested at the rapid strain rate.

Table 11 compares the test results of each of the grouted coupler sleeves specimens to the average results of the as-rolled ASTM 615 Grade 60 control bars tested at the rapid strain rate. Also shown in the table are the average values for each measurement set.
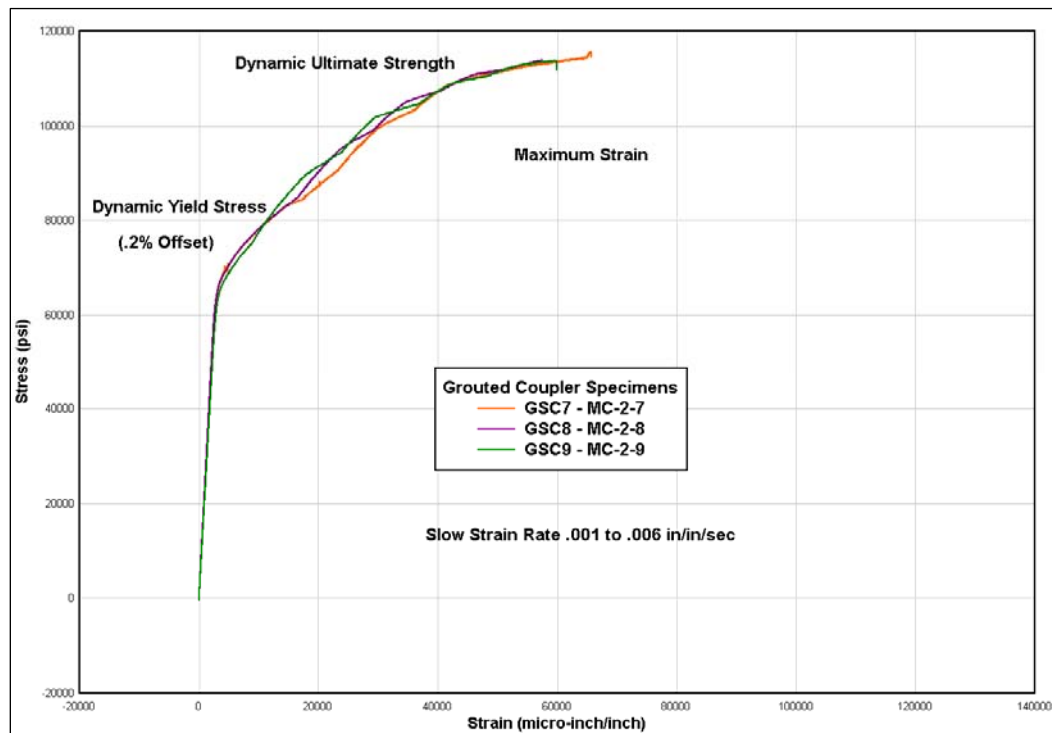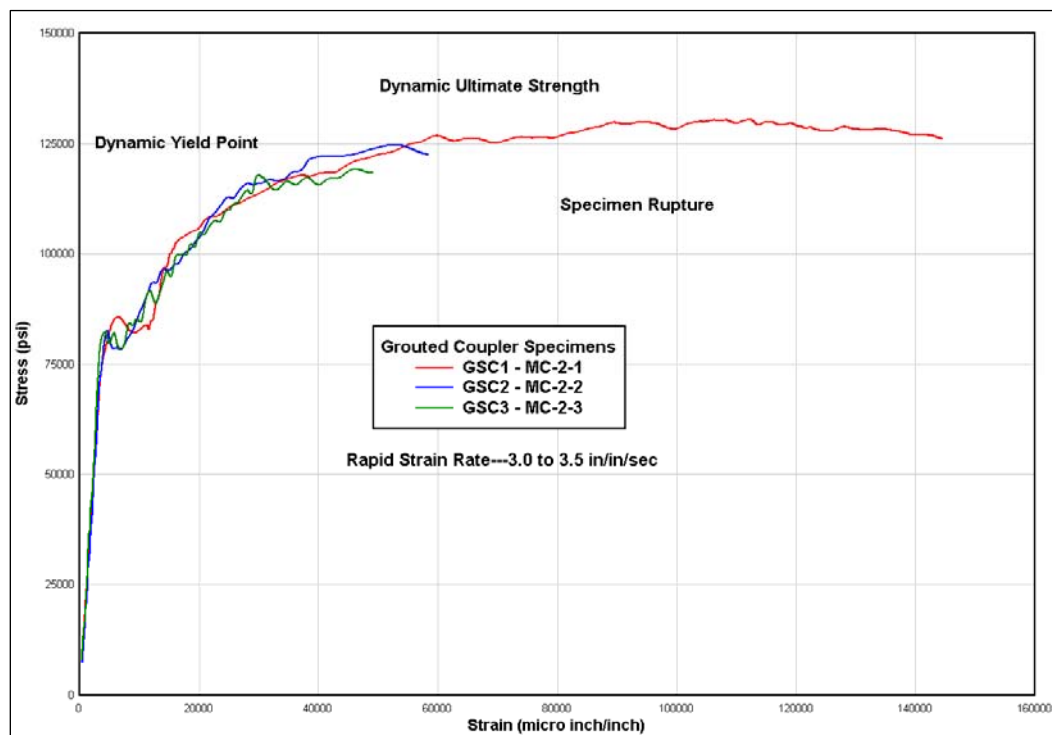
Figure 28. Stress vs. strain for grouted coupler system at the rapid strain rate.

Table 11. Test results of grouted coupler system at rapid strain rates.

Specimen Name	Specimen Number	Yield Point (psi)	Yield Strain (µin./in.)	Dynamic Ultimate Strength (psi)	Maximum Strain (µin./in.)	Ductility Ratio	Elongation %	Strain Rate (in./in./sec)
AR-Rapid	Average	89,800	4,700	129,600	138,000	29.5	13.8	3.2
GSC1	MC-2-1	85,700	6,400	130,300	144,500	22.5	14.5	3.5
GSC2	MC-2-2	82,600	4,600	124,700	58,400	12.7	5.8	3.0
GSC3	MC-2-3	82,300	4,200	119,200	49,000	11.6	4.9	3.2
GSCA	Average	83,600	5,100	124,700	84,000	15.6	8.4	3.2

Shear screw system

Slow strain rate

All three specimens failed in the same failure mode, which was inside the steel coupler at the first shear screw. Specimens SSC7, SSC8, and SSC9 did not develop the required dynamic ultimate tensile strength nor the required ductility of the control bar. Figure 29 shows the three shear screw

Figure 29. Posttest photos of shear screw specimens tested at the slow strain rate.

couplers posttest (right photo) and the indention in the rebar left by the first shear screw (left photo). Failure for all three specimens occurred at this location.

Figure 30 shows stress-strain test results from the shear screw coupler system tested at the slow strain rate.

Figure 30. Stress vs. strain for shear screw coupler system at the slow strain rate.

Table 12 compares the test results of each of the shear screw coupler sleeves to the average results of the as-rolled ASTM 615 Grade 60 control bars tested at the slow strain rate. Also shown in the table are the average values for each measurement set.

Table 12. Test results of shear screw coupler system at slow strain rates.

Specimen Name	Specimen Number	Yield Stress (psi)	Yield Strain (µin./in.)	Dynamic Ultimate Strength (psi)	Maximum Strain (µin./in.)	Ductility Ratio	Elongation %	Strain Rate (in./in./sec)
AR-Slow	Average	70,800	5,200	117,000	100,800	19.4	10.1	0.0037
SSC7	MC-3-7	68,800	5,400	80,600	16,700	3.1	1.7	0.004
SSC8	MC-3-8	69,700	5,000	95,800	27,000	5.4	2.7	0.003
SSC9	MC-3-9	69,300	5,200	81,500	17,600	3.4	1.8	0.004
SSCA	Average	69,300	5,200	86,000	20,400	4.0	2.1	0.004

Intermediate strain rate

All three specimens failed in the same failure mode, which was inside the steel coupler at the first or second shear screw. Specimen SSC4 failed at the second shear screw, and specimens SSC5 and SSC6 failed at the first shear screw. Specimens SSC4 and SSC6 did not develop the required dynamic ultimate tensile strength nor the required ductility of the control bar. Specimen SSC5 almost achieved the required ultimate dynamic tensile stress but did not achieve the required ductility. Figure 31 shows the three shear screw couplers posttest (right photo) and the indention in the rebar left by the second shear screw (left photo). The tip of the first shear screw is still embedded in the rebar.


Figure 31. Posttest photos of shear screw specimens at the intermediate strain rate.

Figure 32 shows the stress-strain test results from each of the shear screw coupler systems tested at the intermediate strain rate. Table 13 compares the test results of the shear screw coupler sleeves to the average results of the as-rolled ASTM 615 Grade 60 control bars tested at the intermediate strain rate. Also shown in the table are the average values of each measurement set.
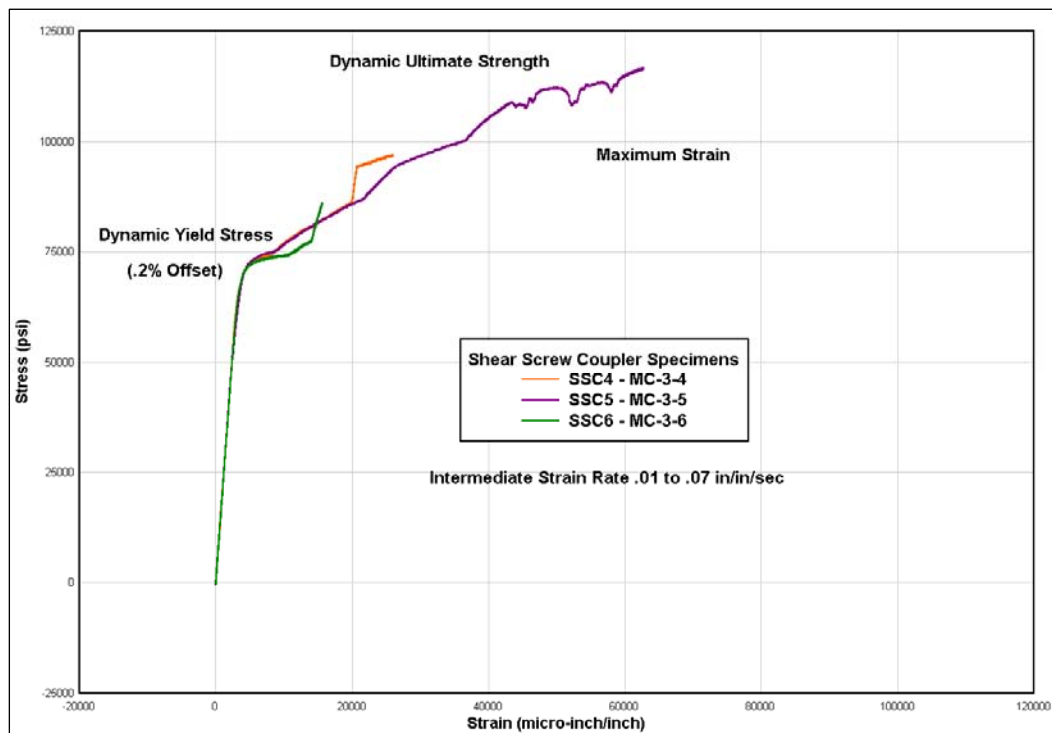
Figure 32. Stress vs. strain for shear screw coupler system at the intermediate strain rate.

Table 13. Test results of shear screw coupler system at intermediate strain rates.

Specimen Name	Specimen Number	Yield Stress (psi)	Yield Strain (μin./in.)	Dynamic Ultimate Strength (psi)	Maximum Strain (μin./in.)	Ductility Ratio	Elongation %	Strain Rate (in./in./sec)
AR-Inter	Average	74,800	5,300	119,500	105,000	19.9	10.5	0.064
SSC4	MC-3-4	72,900	5,600	97,100	26,000	4.7	2.6	0.065
SSC5	MC-3-5	73,300	5,600	116,800	62,800	11.3	6.3	0.062
SSC6	MC-3-6	72,500	5,500	86,200	15,700	2.8	1.6	0.065
SSCA	Average	72,900	5,600	100,000	34,800	6.3	3.5	0.064

Rapid strain rate

The specimens failed in two failure modes. Specimen SSC1 (bottom right in Figure 33) failed by breaking the rebar at the first shear screw, as a result of stress concentration at the deformation in the rebar made by the shear. Specimens SSC2 and SSC3 failed by complete stripout of the rebar from the sleeve. All specimens failed prior to developing the required dynamic ultimate tensile strength and the required ductility.
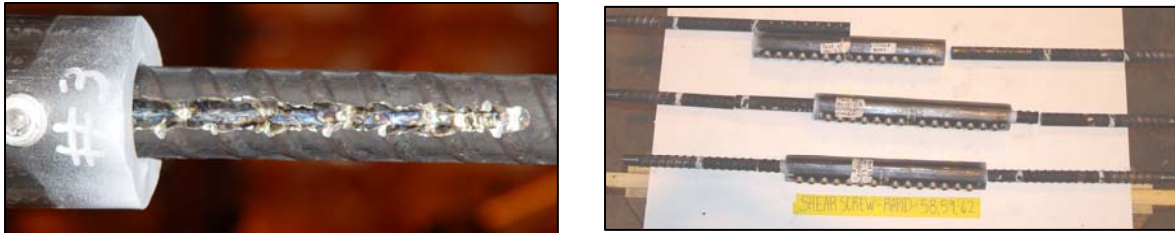
Figure 33. Posttest photos of shear screw specimens tested at the rapid strain rate.

The left photo in Figure 33 shows the indention in the rebar left by the shear screws at stripout. The tips of the shear screw formed a trough embedded in the rebar.

Figure 34 shows the stress-strain test results from the shear screw coupler system tested at the rapid strain rate.
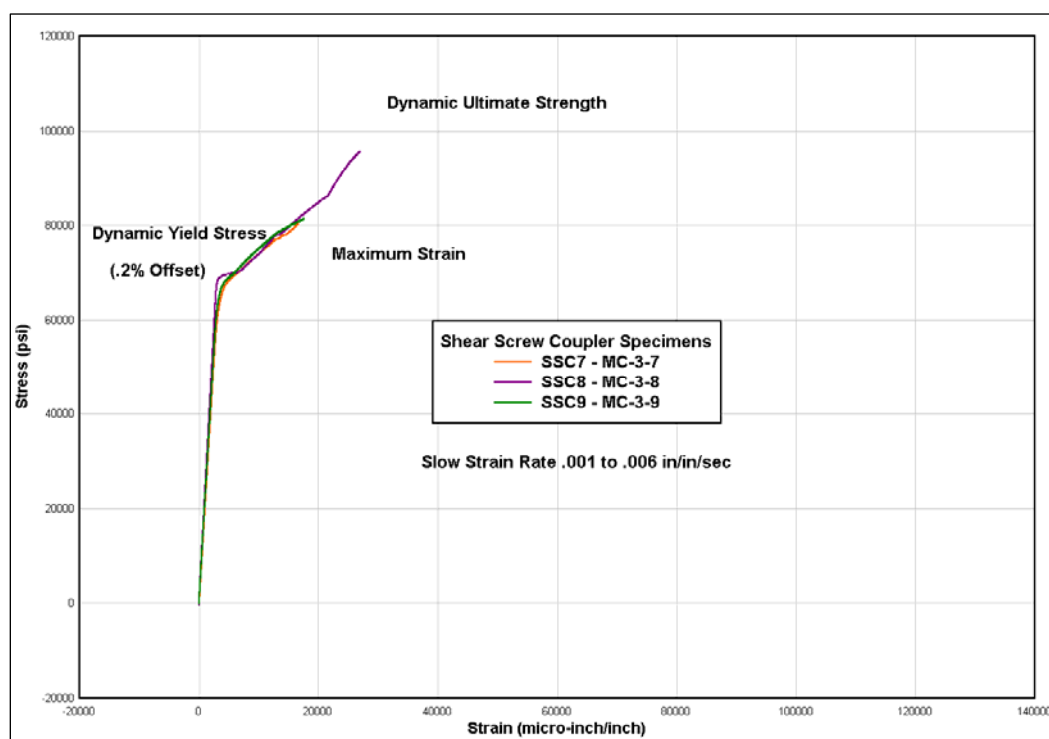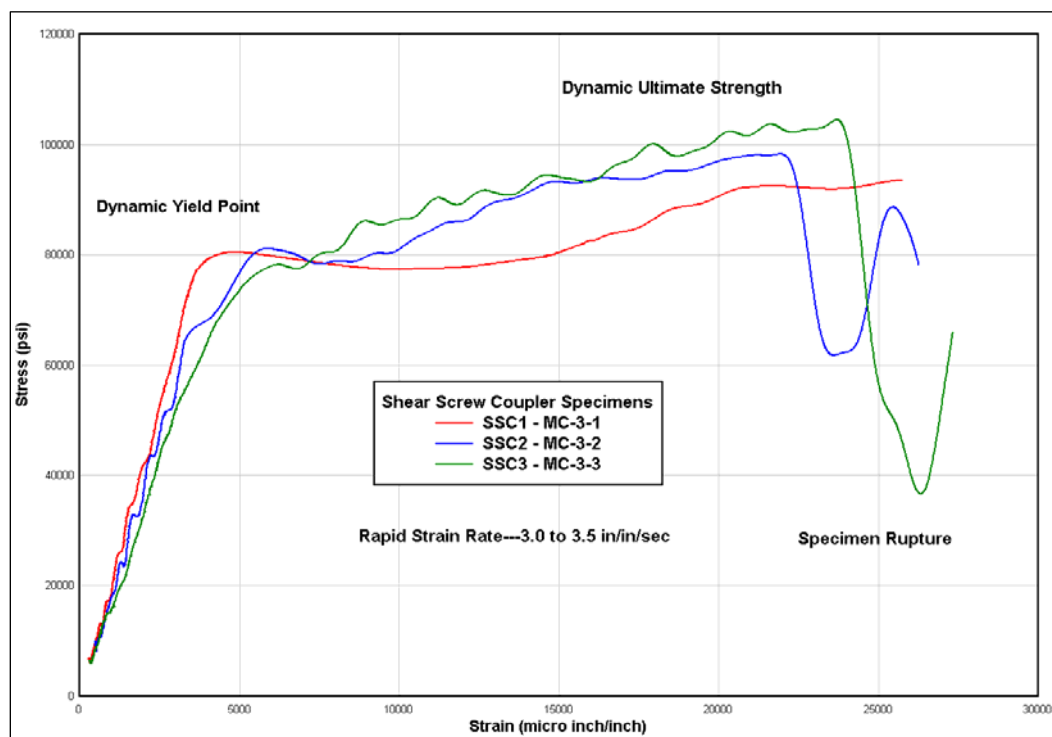

Figure 34. Stress vs. strain for shear screw coupler system at the rapid strain rate.

Table 14 compares the test results of each of the shear screw coupler sleeves to the average results of the as-rolled ASTM 615 Grade 60 control bars tested at the rapid strain rate. Also shown in the table are the average values for each measurement set.

Table 14. Test results of shear screw coupler system at rapid strain rates.

Specimen Name	Specimen Number	Yield Point (psi)	Yield Strain (µin./in.)	Dynamic Ultimate Strength (psi)	Maximum Strain (µin./in.)	Ductility Ratio	Elongation %	Strain Rate (in./in./sec)
AR-Rapid	Average	89,800	4,700	129,600	138,000	29.5	13.8	3.2
SSC1	MC-3-1	80,500	4,800	93,600	25,700	5.3	2.6	3.5
SSC2	MC-3-2	81,100	5,900	98,300	26,300	4.5	2.6	3.2
SSC3	MC-3-3	78,200	6,200	104,500	27,300	4.4	2.7	3.8
SSCA	Average	80,000	5,600	98,800	26,400	4.7	2.6	3.5

Taper threaded system

Slow strain rate

The specimens all failed in the same failure mode, which was failure of the rebar. Specimen TTC7 developed the required ultimate dynamic tensile strength and the required ductility based on the results of the control bar tests. Specimen TTC8 almost developed the ultimate dynamic tensile stress and did achieve the required ductility prior to failure. Specimen TTC9 developed the required dynamic ultimate tensile strength but not the required ductility. Figure 35 shows the three taper threaded couplers posttest (right photo) and the typical mode of failure in the rebar (left photo).

Figure 35. Posttest photos of taper threaded specimens tested at the slow strain rate.

Figure 36 shows the stress-strain test results from the taper threaded coupler system tested at the slow strain rate. Table 15 compares the test results of each of the taper threaded couplers to the average results of the as-rolled ASTM 615 Grade 60 control bars tested at the slow strain rate. Also shown in the table are the average values of each measurement set.

Figure 36. Stress vs. strain for taper threaded coupler system at the slow strain rate.

Table 15. Test results of taper threaded coupler system at slow strain rates.

Specimen Name	Specimen Number	Yield Stress (psi)	Yield Strain (µin./in.)	Dynamic Ultimate Strength (psi)	Maximum Strain (µin./in.)	Ductility Ratio	Elongation %	Strain Rate (in./in./sec)
AR-Slow	Average	70,800	5,200	117,000	100,800	19.4	10.1	0.0037
TTC7	MC-4-7	69,800	5,000	118,000	121,900	23.8	12.2	0.003
TTC8	MC-4-8	66,800	5,000	114,700	121,900	24.4	12.2	0.003
TTC9	MC-4-9	70,700	5,000	118,600	98,200	19.5	9.8	0.003
TTCA	Average	69,100	5,000	117,100	114,000	22.6	11.4	0.003

Intermediate strain rate

The specimens failed in two failure modes. Specimens TTC4 and TTC5 (right bottom and middle, respectively, in Figure 37) failed in the rebar. Specimen TTC6 (top right in Figure 37) failed in the rebar at the last few threads just outside the coupler itself. Specimen TTC5 developed the required ultimate dynamic tensile strength and almost achieved the required ductility. Specimens TTC4 and TTC6 did not develop the ultimate dynamic tensile stress and the required ductility prior to failure. The left photo in Figure 37 shows the typical mode of failure in the rebar.

Figure 37. Posttest photos of taper threaded specimens tested at intermediate strain rate.

Figure 38 shows the stress-strain test results from the taper threaded coupler system tested at the intermediate strain rate. Table 16 compares the test results of the taper threaded couplers to the average results of the as-rolled ASTM 615 Grade 60 control bars tested at the intermediate strain rate. Also shown in the table are the average values of each measurement set.

Figure 38. Stress vs. strain for taper threaded coupler system at intermediate strain rate.

Table 16. Tests results of taper threaded coupler system at intermediate strain rates.

Specimen Name	Specimen Number	Yield Stress (psi)	Yield Strain (µin./in.)	Dynamic Ultimate Strength (psi)	Maximum Strain (µin./in.)	Ductility Ratio	Elongation %	Strain Rate (in./in./sec)
AR-Inter	Average	74,800	5,300	119,500	105,000	19.9	10.5	0.064
TTC4	MC-4-4	73,000	5,100	96,900	25,000	4.9	2.5	0.057
TTC5	MC-4-5	73,300	5,100	120,700	101,800	19.8	10.1	0.058
TTC6	MC-4-6	73,100	5,400	110,200	37,500	6.9	3.8	0.065
TTCA	Average	73,100	5,200	109,200	54,800	10.5	5.5	0.060

Rapid strain rate

All three specimens failed just outside the coupler in the last few threads in the rebar, because of stress concentration at those threads (right photo in Figure 39). All failed prior to developing the dynamic ultimate tensile strength and the required ductility. The left photo in Figure 39 shows the typical mode of failure in the rebar.

Figure 39. Posttest photos of taper threaded specimens tested at rapid strain rate.

Figure 40 shows the stress-strain test results from the taper threaded coupler system tested at the rapid strain rate. Table 17 compares the test results of the taper threaded couplers to the average results of the as-rolled ASTM 615 Grade 60 control bars tested at the rapid strain rate. Also shown in the table are the average values of each measurement set.
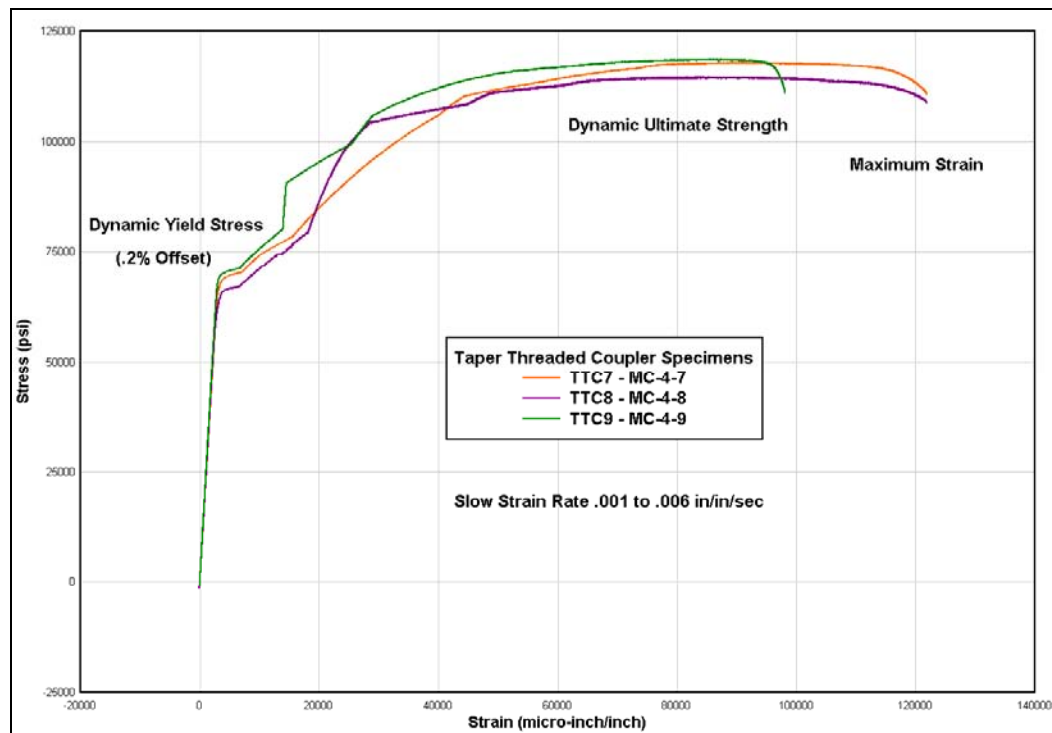
Figure 40. Stress vs. strain for taper thread coupler system at the rapid strain rate.

Table 17. Test results of taper thread coupler system at rapid strain rates.

Specimen Name	Specimen Number	Yield Stress (psi)	Yield Strain (μin./in.)	Dynamic Ultimate Strength (psi)	Maximum Strain (μin./in.)	Ductility Ratio	Elongation %	Strain Rate (in./in./sec)
AR-Rapid	Average	89,800	4,700	129,600	138,000	29.5	13.8	3.2
TTC1	MC-4-1	86,400	5,900	87,800	13,300	2.3	1.3	3.0
TTC2	MC-4-2	86,900	5,700	106,000	24,300	4.3	2.4	3.0
TTC3	MC-4-3	86,300	4,400	102,400	19,700	4.5	2.0	3.7
TTCA	Average	86,500	5,300	98,800	19,100	3.7	1.9	3.2

Threaded rebar coupler system

Slow strain rate

The specimens all failed in the same failure mode, which was in the rebar. During the test on specimen TBC7, the dynamic loader was not properly pressurized to provide sufficient stroke to fail the specimen in one run. Therefore, the test was divided into three separate runs until failure occurred. This created a nonstandard test result that cannot be compared

to the results of the other specimens. Specimens TBC8 and TBC9 both developed the required ultimate dynamic tensile strength but did not achieve the required ductility. Figure 41 shows the three threaded bar couplers posttest (right photo) and a typical mode of failure in the rebar (left photo).

Figure 41. Posttest photos of threaded bar specimens tested at slow strain rate.

Figure 42 shows the stress-strain test results from the threaded bar coupler system tested at the slow strain rate.

Figure 42. Stress vs. strain for threaded rebar coupler system at the slow strain rate.

Table 18 compares the test results of the threaded bar couplers to the average results of the as-rolled ASTM 615 Grade 75 control bars tested at the slow strain rate. Also shown in the table are the average values for each measurement set.
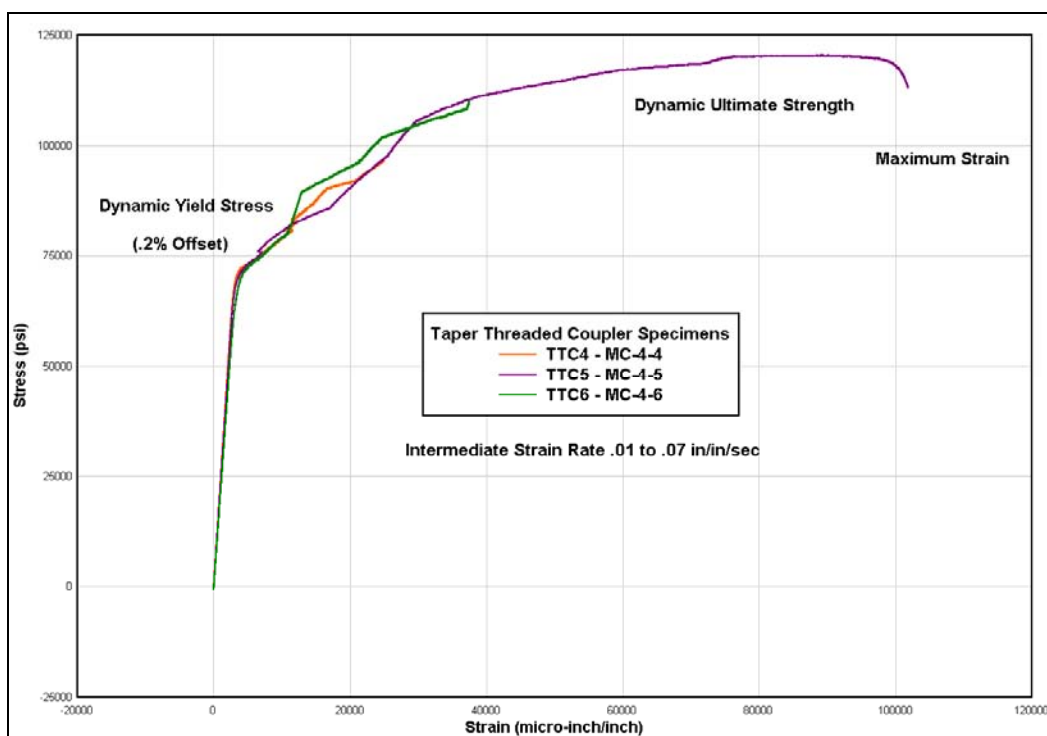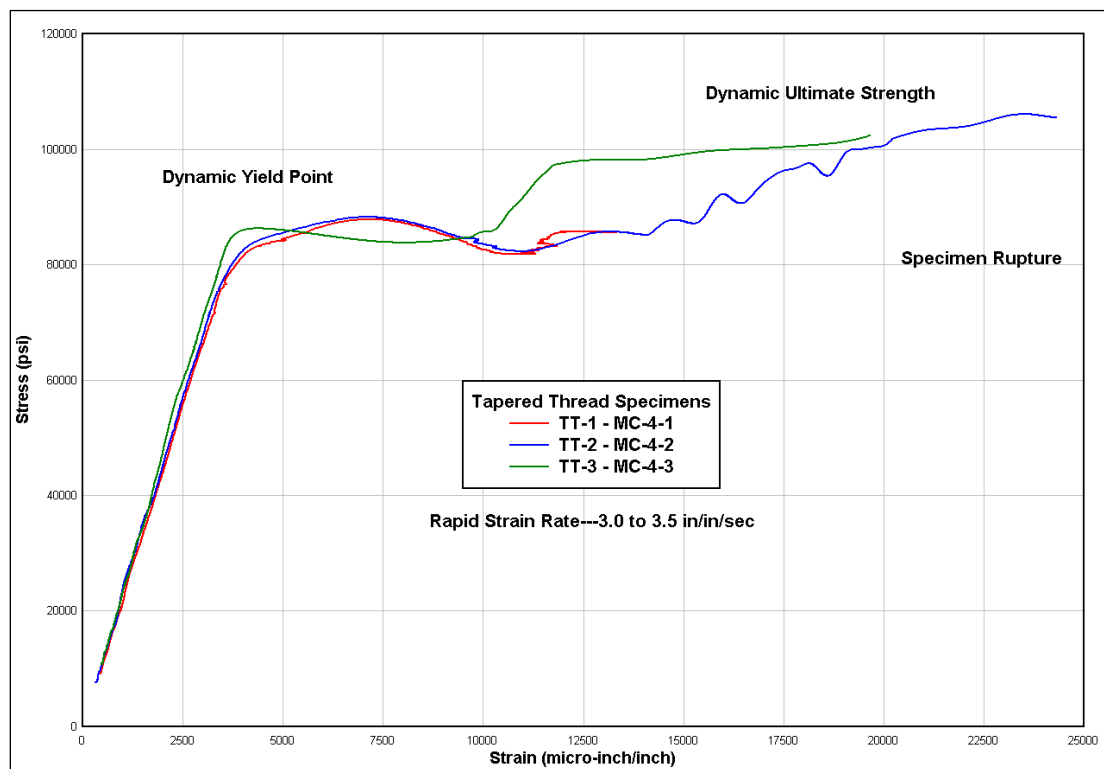
Table 18. Test results of threaded rebar coupler system at slow strain rates.

Specimen Name	Specimen Number	Yield Point (psi)	Yield Strain (µin./in.)	Dynamic Ultimate Strength (psi)	Maximum Strain (µin./in.)	Ductility Ratio	Elongation %	Strain Rate (in./in./sec)
ART-Slow	Average	76,100	4,000	110,400	108,600	27.5	10.9	0.0031
TBC7	MC-5-7	-----	-----	-----	-----	-----	-----	-----
TBC8	MC-5-8	80,300	4,500	111,500	69,000	15.2	6.9	0.003
TBC9	MC-5-9	80,900	3,400	111,700	65,900	19.6	6.5	0.003
TBCA	Average	80,600	3,900	111,600	67,400	17.4	6.7	0.003

Intermediate strain rate

All three specimens failed in the same failure mode, which was in the rebar (right photo in Figure 43). All specimens almost achieved the dynamic ultimate tensile strength of the control bar; none achieved the required ductility prior to failure. The left photo in Figure 43 shows a typical mode of failure in the rebar.
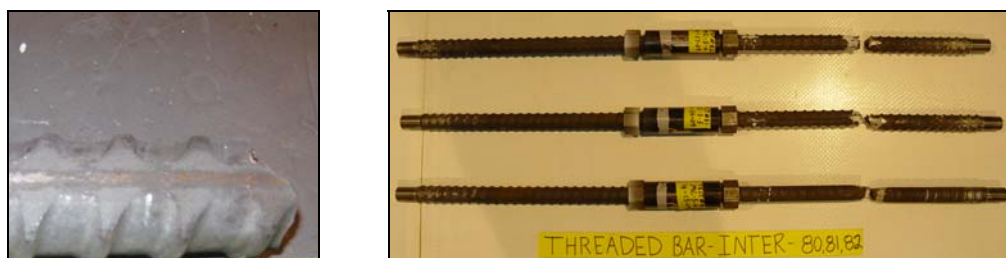
Figure 43. Posttest photos of threaded bar specimens tested at intermediate strain rate.

Figure 44 shows the stress-strain test results from the threaded bar coupler system tested at the intermediate strain rate.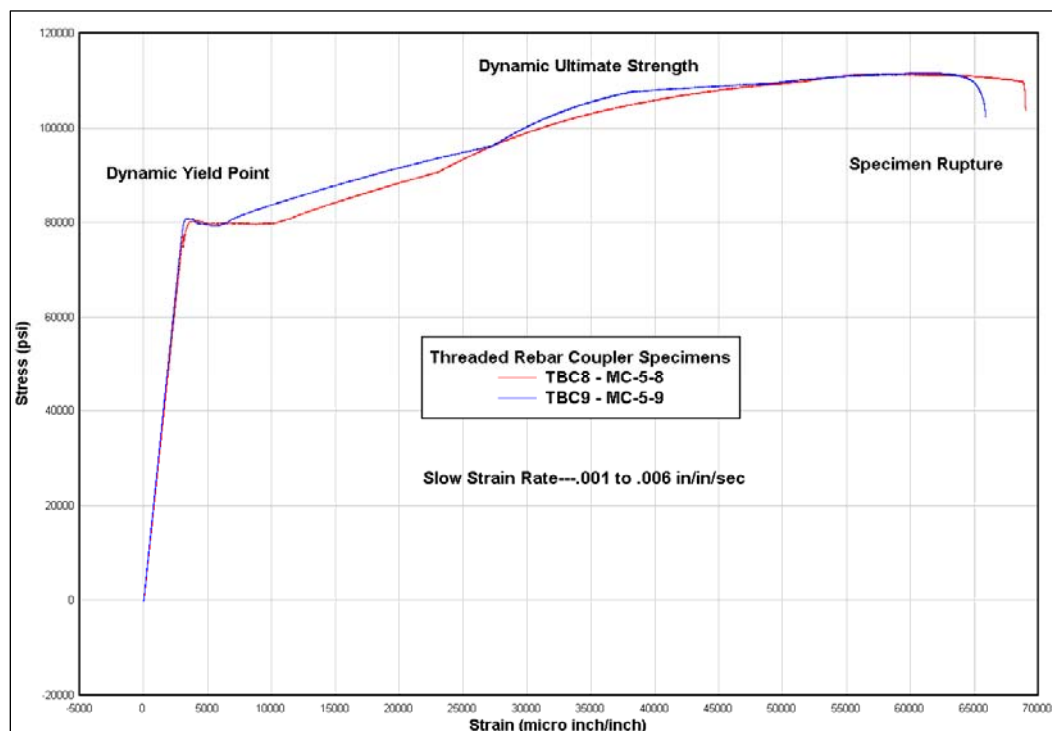 Table 19 compares the test results of the threaded bar couplers to the average results of the as-rolled ASTM 615 Grade 75 control bars tested at the intermediate strain rate. Also shown in the table are the average values for each measurement set.

Figure 44. Stress vs. strain for threaded rebar coupler system at the intermediate rate.

Table 19. Test results of threaded rebar coupler system at intermediate strain rates.

Specimen Name	Specimen Number	Yield Point (psi)	Yield Strain (µin./in.)	Dynamic Ultimate Strength (psi)	Maximum Strain (µin./in.)	Ductility Ratio	Elongation %	Strain Rate (in./in./sec)
ART-Inter	Average	81,500	3,800	115,200	115,200	31.0	11.5	0.052
TBC4	MC-5-4	80,900	4,100	113,700	109,900	26.9	11.0	0.048
TBC5	MC-5-5	80,700	3,700	113,300	109,100	29.4	10.9	0.050
TBC6	MC-5-6	81,200	4,900	113,900	92,900	19.0	9.3	0.050
TBCA	Average	80,900	4,200	113,700	104,000	25.1	10.4	0.049

Rapid strain rate

All three specimens failed in the rebar (right photo in Figure 45). Specimen TBC1 almost achieved the dynamic ultimate tensile strength of the control bar but did not achieve the required ductility prior to failure. Specimen TBC2 achieved the required dynamic ultimate tensile strength of the control bar; however, it did not achieve the required ductility prior to failure.
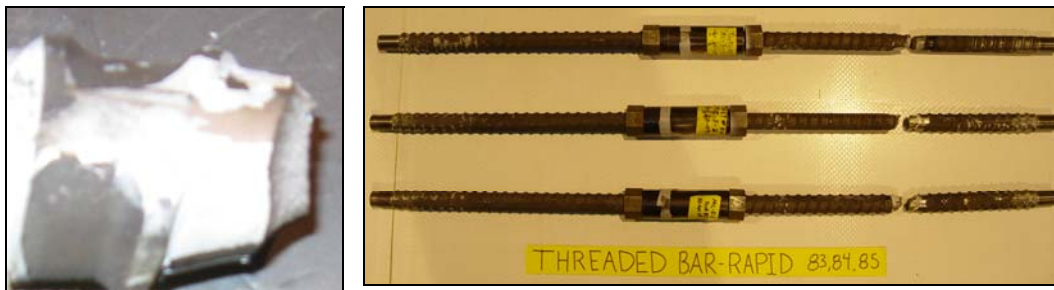
Figure 45. Posttest photos of threaded bar specimens tested at rapid strain rate.

Specimen TBC3 achieved both the required dynamic ultimate tensile strength and the required ductility of the control bar prior to failure. The left photo in Figure 45 shows a typical mode of failure in the rebar.

Figure 46 shows the stress-strain test results from the threaded bar coupler system tested at the rapid strain rate. Table 20 compares the test results of the threaded bar couplers to the average results of the as-rolled ASTM 615 Grade 75 control bars tested at the rapid strain rate. Also shown in the table are the average values for each measurement set.
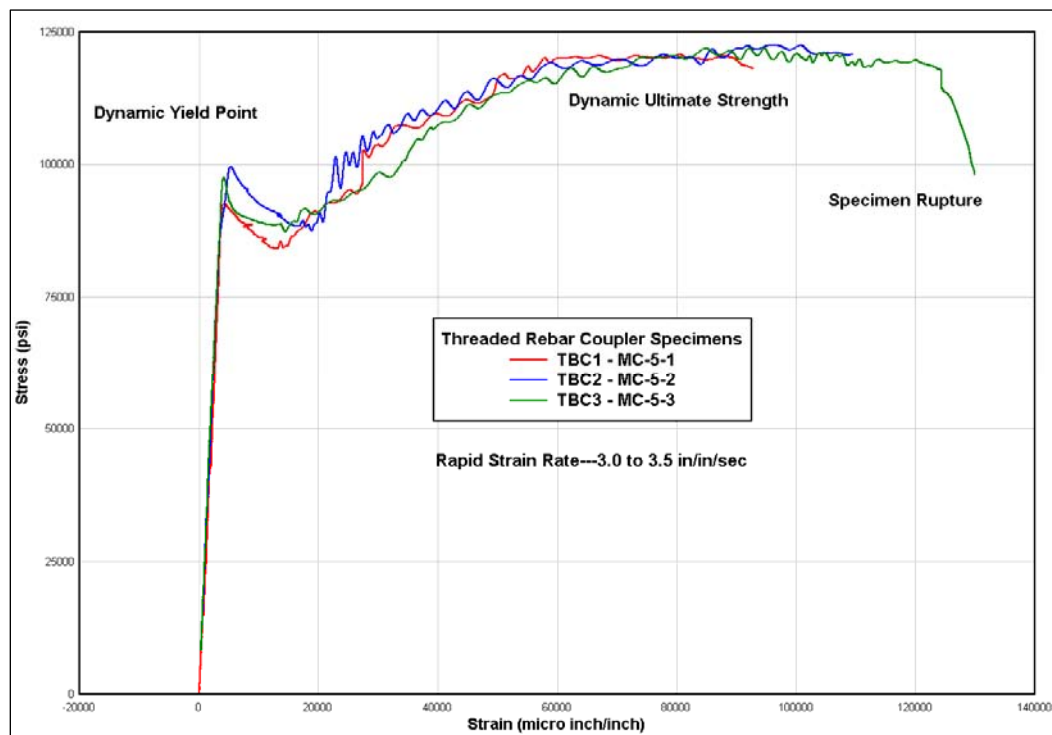
Figure 46. Stress vs. strain for threaded rebar coupler system at the rapid strain rate.

Table 20. Test results of threaded rebar coupler system at rapid strain rates.
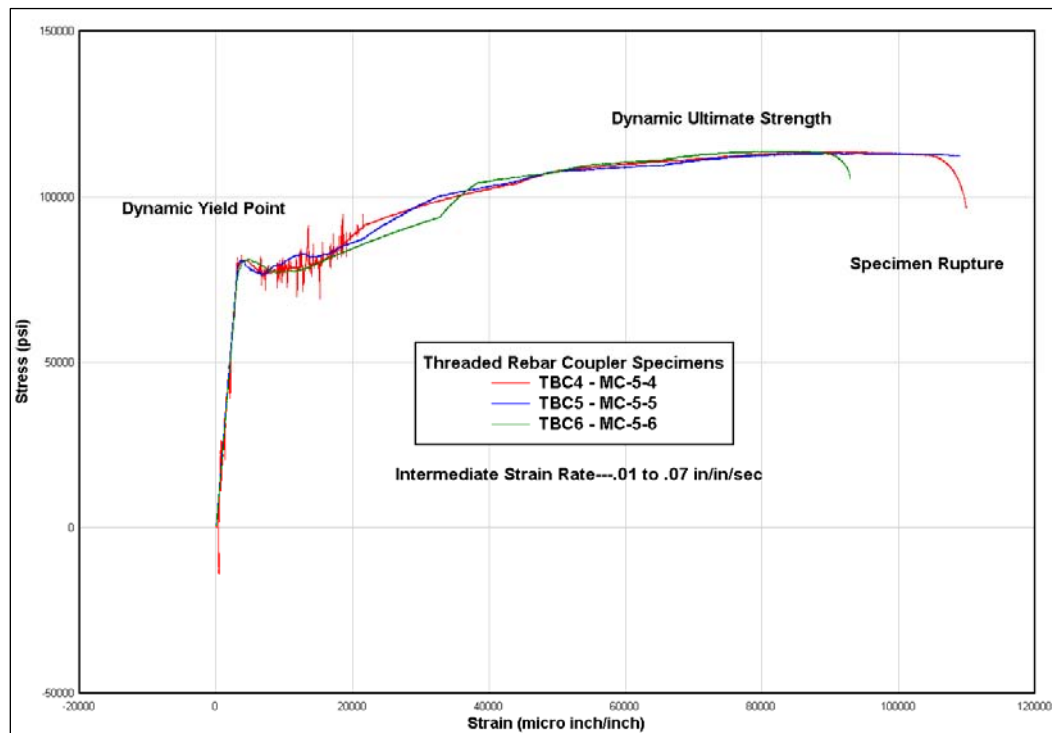
Specimen Name	Specimen Number	Yield Point (psi)	Yield Strain (µin./in.)	Dynamic Ultimate Strength (psi)	Maximum Strain (µin./in.)	Ductility Ratio	Elongation %	Strain Rate (in./in./sec)
ART-Rapid	Average	99,000	4,000	122,800	122,000	30.2	12.2	3.2
TBC1	MC-5-1	92,600	4,400	120,900	92,900	21.2	9.3	3.2
TBC2	MC-5-2	99,700	5,300	122,500	109,700	21.7	11.0	3.4
TBC3	MC-5-3	97,700	4,200	122,000	130,000	31.1	12.9	3.3
TBCA	Average	96,400	4,600	121,800	110,800	24.7	11.1	3.3

4   Data Analysis

As-rolled ASTM 615 Grade 60 control bars

Army Manual TM 5-855-1 (Department of the Army et al. 1998) provides design curves for dynamic increase factors (DIFs) for several grades of steel versus strain rate. These factors allow the designer to account for the increase in yield and ultimate strengths due to the high strain-rate effects associated with dynamic loading conditions. Figure 4-48 of TM 5-855-1 gives the DIFs for ASTM 615 Grades 40 and 60 steel. If the DIFs found in TM 5-855-1 for Grade 60 are divided into the dynamic yield stress and dynamic ultimate tensile strengths determined by the slow strain-rate tests, the results will give the static yield stress and tensile strength of the material. Once these values are determined, the DIFs can be applied to these static values to determine the dynamic yield stress and dynamic ultimate tensile strength for the intermediate and rapid strain rates. A comparison of these calculated values for the intermediate and rapid strain rates with the data collected from the as-rolled control Grade 60 bars conducted under this effort (Table 3) is presented in Table 21. This confirms that the results of the control bar test are valid and comparable to historical data.

Table 21. Application of DIFs to ASTM 615 Grade 60 as-rolled control bars.

Strain Rate (in./in./sec)	DIF Yield	DIF Ultimate	Yield Stress Calculated (psi)	Yield Stress Experimental (psi)	Ultimate Stress Calculated (psi)	Ultimate Stress Experimental (psi)
Static	1	1	62,700	-----	114,700	-----
0.004	1.13	1.02	70,800	70,800	117,000	117,000
0.064	1.21	1.04	75,900	74,800	119,300	119,500
3.2	1.43	1.09	89,700	89,800	125,000	129,600

Machined ASTM 615 Grade 60 bars

The same analysis performed on the as-rolled control bars can be applied to the material properties obtained from the results of the machined bar tests. The analysis results are shown in Table 22 and seem to agree with

Table 22. Application of DIF's to ASTM 615 Grade 60 machined bars.

Strain Rate (in./in./sec)	DIF Yield	DIF Ultimate	Yield Stress Calculated (psi)	Yield Stress Experimental (psi)	Ultimate Stress Calculated (psi)	Ultimate Stress Experimental (psi)
Static	1	1	64,500	-----	121,500	-----
0.002	1.13	1.02	72,900	72,900	123,900	123,900
0.067	1.21	1.04	78,000	75,800	126,400	125,600
3.49	1.43	1.09	92,200	98,800	132,400	143,800

the DIFs with the exception of an approximate 8% increase in the experimental high strain-rate results.

As-rolled ASTM 615 Grade 75 control bars

No DIFs were available for the ASTM 615 Grade 75 control bars. Therefore, a comparison of the test results for as-rolled Grade 60 and Grade 75 bars is provided in Table 23.

Table 23. Comparison of test results for ASTM 615 Grade 60 and Grade75 control bars.

Strain Rate (in./in./sec)	ASTM 615 Grade	Yield Point (psi)	Yield Strain (μin./in.)	Dynamic Ultimate Strength (psi)	Maximum Strain (μin./in.)	Ductility Ratio	Elongation %
0.004	60	70,800	5,200	117,000	100,800	19.4	10.1
0.003	75	76,100	4,000	110,400	108,600	27.5	10.9
		+7%	-23%	-6%	+7%	+29%	+7%
0.064	60	74,800	5,300	119,500	105,000	19.9	10.5
0.052	75	81,500	3,800	115,200	115,000	31.0	11.5
		+8%	-28%	-4%	+9%	+36%	+9%
3.2	60	89,800	4,700	129,600	138,000	29.5	13.8
3.2	75	99,000	4,000	122,800	122,000	30.2	12.2
		+9%	-15%	-5%	-12%	+2%	-12%

The results in Table 23 indicate that the yield points for the Grade 75 bar at all strain rates are higher than those for the Grade 60 bar tested at comparable strain rates. However, the yield strains for the Grade 75 bars are less at all three strain rates than those for the Grade 60 bar. This indicates that the Grade 75 bar is stronger and less ductile at the yield point than the Grade 60 bar at all three strain rates. In terms of dynamic

ultimate strength and maximum strain, the Grade 75 bar has lower
strength and higher strains at the slow and intermediate rates. However,
at the rapid rate, the Grade 75 bar has both lower dynamic ultimate
strengths and lower maximum strains compared with the Grade 60 bar.
These ultimate strengths and maximum strains are somewhat counter to
those at yield. The data imply that, although stronger and less ductile at
yield, the Grade 75 bars have less strength and are generally more ductile
at the ultimate point compared with the responses of the Grade 60 bar.
Finally, at all three strain rates, the Grade 75 bar has a higher ductility
than the Grade 60 bar, but only slightly so at the rapid rate.

Upset head system

The upset head coupler (UHC) system performed very well under the slow
strain-rate loading conditions. The system developed on average 102% of
the dynamic ultimate tensile strength, 106% of the maximum strain, and
110% of the ductility achieved by the control bar. The mode of failure for
all three specimens was in the rebar outside the heat-affected zone.

The average performance of the UHC system under the intermediate
strain-rate loading condition produced 99% of the dynamic ultimate
strength, 61% of the maximum strain, and 60% of the ductility achieved by
the control bar. One specimen failed outside the heat-affected zone while
the other two specimens failed in the heat-affected zone. One of the latter
two specimens failed just under the upset head. Failures inside the heat-
affected zone exhibited a brittle failure with little to no necking.

Under the rapid strain-rate loading condition, the UHC system developed
an average of 90% of the dynamic ultimate strength, 50% of the maximum
strain, and 49% of the ductility achieved by the control bar. One specimen
failed outside the heat-affected zone while the other two specimens failed
in the heat-affected zone, with one of the latter two specimens failing just
under the upset head.

Table 24 contains individual specimen performances as well as the average
UHC system performance.

Table 24. Percent of response of mechanical coupler system compared to response of as-rolled control bars.

Specimen Name	Slow Strain Rate			Intermediate Strain Rate			Rapid Strain Rate		
	Dynamic Ultimate Strength	Maximum Strain	Ductility Ratio	Dynamic Ultimate Strength	Maximum Strain	Ductility Ratio	Dynamic Ultimate Strength	Maximum Strain	Ductility Ratio
UHC – Upset Head System									
1	-----	-----	-----	101	73	70	75	15	12
2	102	111	115	100	67	68	100	96	86
3	102	101	104	95	43	43	95	39	48
Average	102	106	110	99	61	60	90	50	49
GSC – Grouted Sleeve Coupler System									
1	99	65	64	102	85	81	101	105	76
2	97	57	60	102	82	80	96	42	43
3	97	59	60	102	78	77	92	36	39
Average	98	61	61	102	82	79	96	61	53
SSC – Shear Screw Coupler System									
1	69	17	16	81	25	24	72	19	18
2	82	27	28	98	60	57	76	19	15
3	70	17	18	72	15	14	81	20	15
Average	73	20	21	84	33	32	76	19	16
TTC – Tapered Thread Coupler System									
1	101	121	123	81	24	25	68	10	8
2	98	121	126	101	96	99	82	18	15
3	101	97	101	92	36	35	79	14	15
Average	100	113	116	91	52	53	76	14	13
TBC – Threaded Rebar Coupler System									
1	-----	-----	----	99	95	88	98	76	70
2	101	64	55	98	95	95	100	90	72
3	101	61	71	99	81	61	99	106	103
Average	101	62	63	99	90	81	99	91	82

The couplers themselves performed very well under all three strain rates. No couplers were observed to fail within the coupler connection itself. Failure for this system occurred either within the rebar heat-affected zone or in the rebar just outside the heat-affected zone. Couplers subjected to the slow- and intermediate-strain rates could be disassembled posttest. Couplers subjected to the high strain rate could not be disassembled posttest, which indicated deformation of the internal threads in the male-female threaded connection.

Grouted sleeve coupler system

The grouted sleeve coupler (GSC) system on average under the slow-strain rate loading condition developed 99% of the dynamic ultimate tensile strength, 61% of the maximum strain, and 61% of the ductility achieved by the control bar (see Table 24). One GSC specimen failed as a result of pullout of the rebar from the grouted sleeve, and the other two failed in the sleeve at the midpoint of the sleeve. It is undetermined why the pullout failure occurred. The failure at the sleeve midpoint was due to voids and imperfections in the cast steel grout sleeve.

The performance of the GSC system under the intermediate-strain rate loading condition developed on average 102% of the dynamic ultimate strength, 82% of the maximum strain, and 79% of the ductility achieved by the control bar (see Table 24). Two specimens failed in the bar outside the cast steel grout sleeve, while the third failed at the midpoint of the cast steel grout sleeve, as the result of stress concentration at voids caused during the casting process.

The GSC system under the rapid-strain rate loading condition developed on average 96% of the dynamic ultimate strength, 61% of the maximum strain, and 53% of the ductility achieved by the control bar (see Table 24). One specimen failed because of rebar pullout; one specimen failed in the rebar outside the grout sleeve; and one specimen failed because of a violent failure of the cast steel grout sleeve.

Shear screw coupler system

The shear screw coupler (SSC) system under the slow-strain rate loading condition developed on average 73% of the dynamic ultimate tensile strength, 20% of the maximum strain, and 21% of the ductility achieved by the control bar (see Table 24). All three specimens failed in the rebar at the first shear screw location just inside the steel coupler sleeve.

The SSC system under the intermediate-strain rate loading condition developed on average 84% of the dynamic ultimate strength, 33% of the maximum strain, and 32% of the ductility achieved by the control bar (see Table 24). All three specimens failed in the rebar at the first or second shear screw location just inside the steel coupler sleeve.

The SSC system average performance under the rapid-strain rate loading condition developed on average 76% of the dynamic ultimate strength, 19% of the maximum strain, and 16% of the ductility achieved by the control bar (see Table 24). Failure occurred in two modes. Two specimens failed by complete stripout of the rebar from the coupler sleeve, and one specimen failed in the rebar at the first shear screw location just inside the steel sleeve.

All steel sleeves performed very well. However, the stress concentration in the rebar caused by the tip of the shear screw embedded in the rebar caused premature failure prior to development of the required dynamic ultimate tensile strength and the required maximum strain.

Taper threaded coupler system

The taper threaded coupler (TTC) system performed very well under the slow-strain rate loading conditions. The system developed on average 100% of the dynamic ultimate tensile strength, 113% of the maximum strain, and 116% of the ductility achieved by the control bar (see Table 24). All three specimens failed under in the rebar after achieving the required dynamic ultimate strength and maximum strain.

Under the intermediate-strain rate loading condition, the TTC developed on average 91% of the dynamic ultimate strength, 52% of the maximum strain, and 53% of the ductility achieved by the control bar (see Table 24). Two specimens failed in the rebar outside the taper threads, and one specimen failed in the rebar in the last threads of the taper thread, as a result of the stress concentration caused by the taper threads in the rebar.

Under the rapid-strain rate loading, the TTC system developed on average 76% of the dynamic ultimate strength, 14% of the maximum strain, and 13% of the ductility achieved by the control bar (see Table 24). All three specimens failed in the rebar in the last threads of the taper thread as a result of the stress concentration caused by the taper threads in the rebar.

The couplers themselves performed very well under all three strain rates. No couplers were observed to fail within the coupler connection itself. Failure for this system occurred either within the rebar outside the threads or in the rebar in the last of the taper threads. Couplers subjected to all three strain rates could be disassembled posttest, indicating no

detrimental deformation of the internal threads in the male-female threaded connection.

Threaded bar coupler system

The threaded bar coupler (TBC) system under the slow-strain rate loading condition developed on average 101% of the dynamic ultimate tensile strength, 62% of the maximum strain, and 63% of the ductility achieved by the control bar (see Table 24). All three specimens failed in the rebar outside the coupler.

The TBC system under the intermediate-strain rate loading condition developed on average 99% of the dynamic ultimate strength, 90% of the maximum strain, and 81% of the ductility achieved by the control bar (see Table 24). All three specimens failed in the rebar outside the coupler.

The TBC system under the rapid-strain rate loading condition developed on average 99% of the dynamic ultimate strength, 91% of the maximum strain, and 82% of the ductility achieved by the control bar (see Table 24). All three specimens failed in the rebar outside the coupler.

The couplers themselves performed very well under all three strain rates. No couplers were observed to fail within the coupler connection itself. Failure for this system occurred in the rebar outside of the coupler. Couplers subjected to all three strain rates could be disassembled posttest, indicating no detrimental deformation of the internal threads in the threaded bar connection. Minor deformation was observed posttest when the couplers were disassembled.

5   Summary and Recommendations

Summary

All coupler sleeves with the exception of the grouted sleeve performed very well. The cast-steel grout sleeve was the only sleeve that failed. Most failures that occurred appeared to be the result of the process required to prepare or make the mechanical connections. For example, the upset head failed in the heat-affected zone. The shear screw failed at the first or second shear screw embedment. The taper threaded coupler failed at the last taper threads just outside the coupler itself. The only coupler system that did not exhibit this type of failure was the threaded bar coupler.

Many of the couplers had successful or near-successful individual test results. However, when combined with the rest of the results of the other couplers within the series, the average results of the series were less than the requirements.

The taper thread coupler and the upset head coupler met the requirements at the slow strain rate and are candidates for use in hardened structures subjected to the slow strain rates such as reported herein.

The threaded rebar coupler and the grouted sleeve coupler performed the best compared with the other couplers at the intermediate rate. The TBC developed 99% of the dynamic ultimate tensile strength (DUTS), 90% of the maximum strain (MS), and 81% of the ductility ration (DR) of the control bar. The GSC developed 102% of the DUTS, 82% of the MS, and 79% of the DR of the control bar.

The TBC performed the best compared with the other couplers at the high strain rate. It developed 99% of the DUTS, 91% of the MS, and 81% of the DR of the control bar.

The detailed test procedure described in this report provides a basis for an open test procedure for these types of mechanical couplers.

Recommendations

The threaded bar coupler should be further investigated and additional tests conducted at all three strain rates to provide additional test results for review.

The standard lap splice specified in the TM 5-1300 should be tested experimentally in the same manner and at the same strain rates as performed on mechanical couplers in this effort, and the results compared with the performances of the control bars and the mechanical couplers documented herein.

The upset head, grout sleeve, and threaded rebar couplers should be tested in either subscale or full-scale reinforced concrete slabs at strain rates similar to those used in this study to determine their performances when combined with concrete cover. The subscale tests could be conducted in the ERDC blast load simulator. Full-scale tests could be conducted in the field. This group of couplers should also be modeled using a finite element code so that comparisons can be made between experimental results and analytical results obtained through the high performance computational models. These models could also be used to validate and extrapolate results so that optimum designs can be evaluated without costly field experiments.

Although system failures occurred at lower capacity than the control bars, the failure occurred in the rebar and not in the coupler. Therefore, consideration should be given to modification of the failure and acceptance criteria.

References

American Concrete Institute (ACI). 2002. Building code requirements for structural concrete. ACI Report 318-02, Farmington Hills, MI.

_____. 2007. Types of mechanical splices for reinforcing bars. ACI Report 439.3R-07. Farmington Hills, MI.

Departments of the Army, Navy, and Air Force. 1990. Structures to resist the effects of accidental explosions. Department of the Army Technical Manual TM 5-1300; Department of the Navy Publication NAVFAC P-397; Department of the Air Force Manual AFR 88-22. Washington DC.

Departments of the Army, Navy, and Air Force and the Defense Special Weapons Agency. 1998. Design and analysis of hardened structures to conventional weapons effects. Department of the Army Technical Manual TM 5-855-1; Department of the Navy Publication NAVFAC P-1080; Department of the Air Force Manual AFPAM 32 1147(I). Washington DC.

Flathau, W. J. 1971. Dynamic tests of large reinforcing bar splices. Technical Report N--71-2. Vicksburg, MS: U.S. Army Engineer Waterways Experiment Station.

Huff, W. L. 1969. Test devices, Blast Load Generator Facility. Miscellaneous Paper N-69-1, Vicksburg, MS: U.S. Army Engineer Waterways Experiment Station.
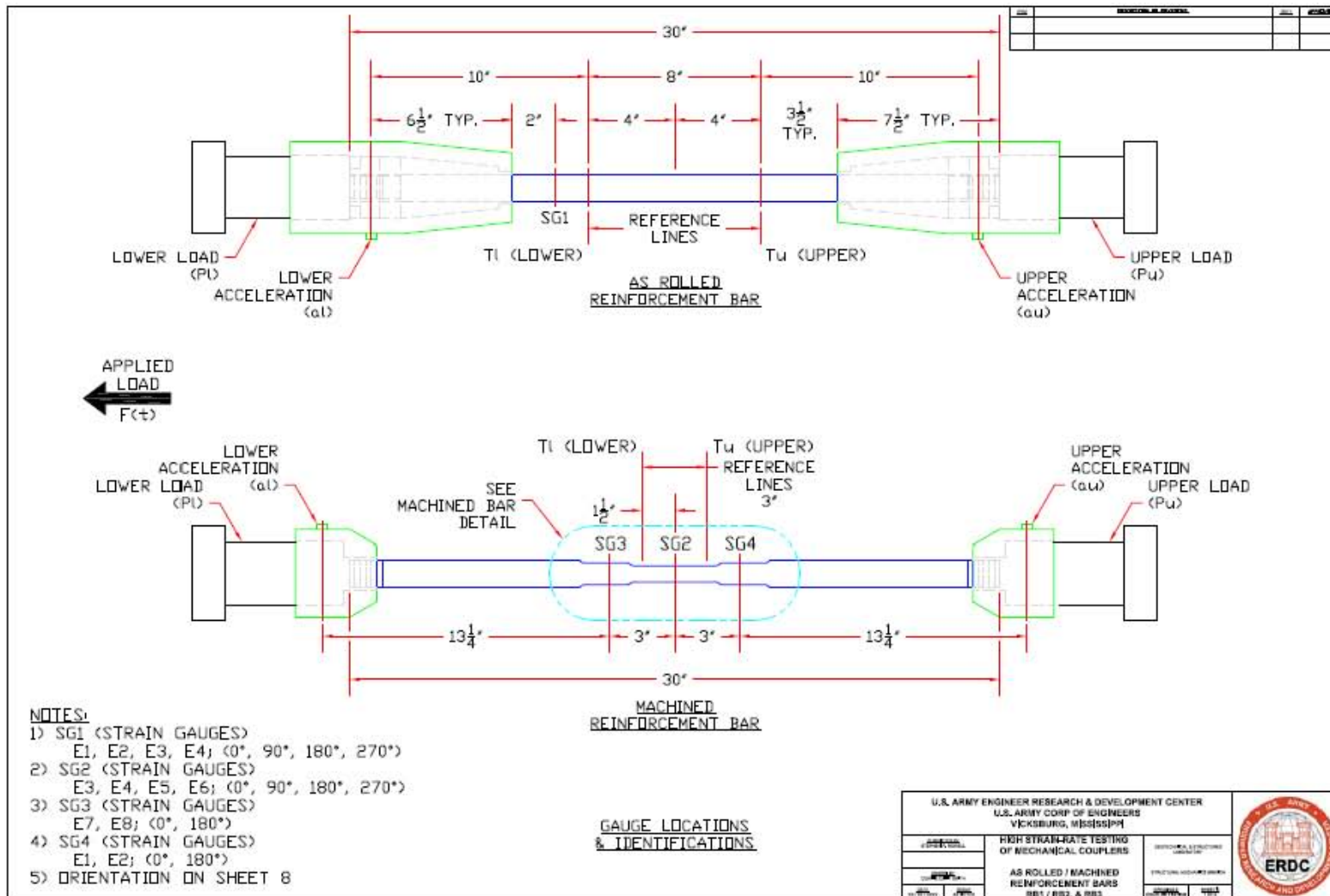
Appendix A: Drawings

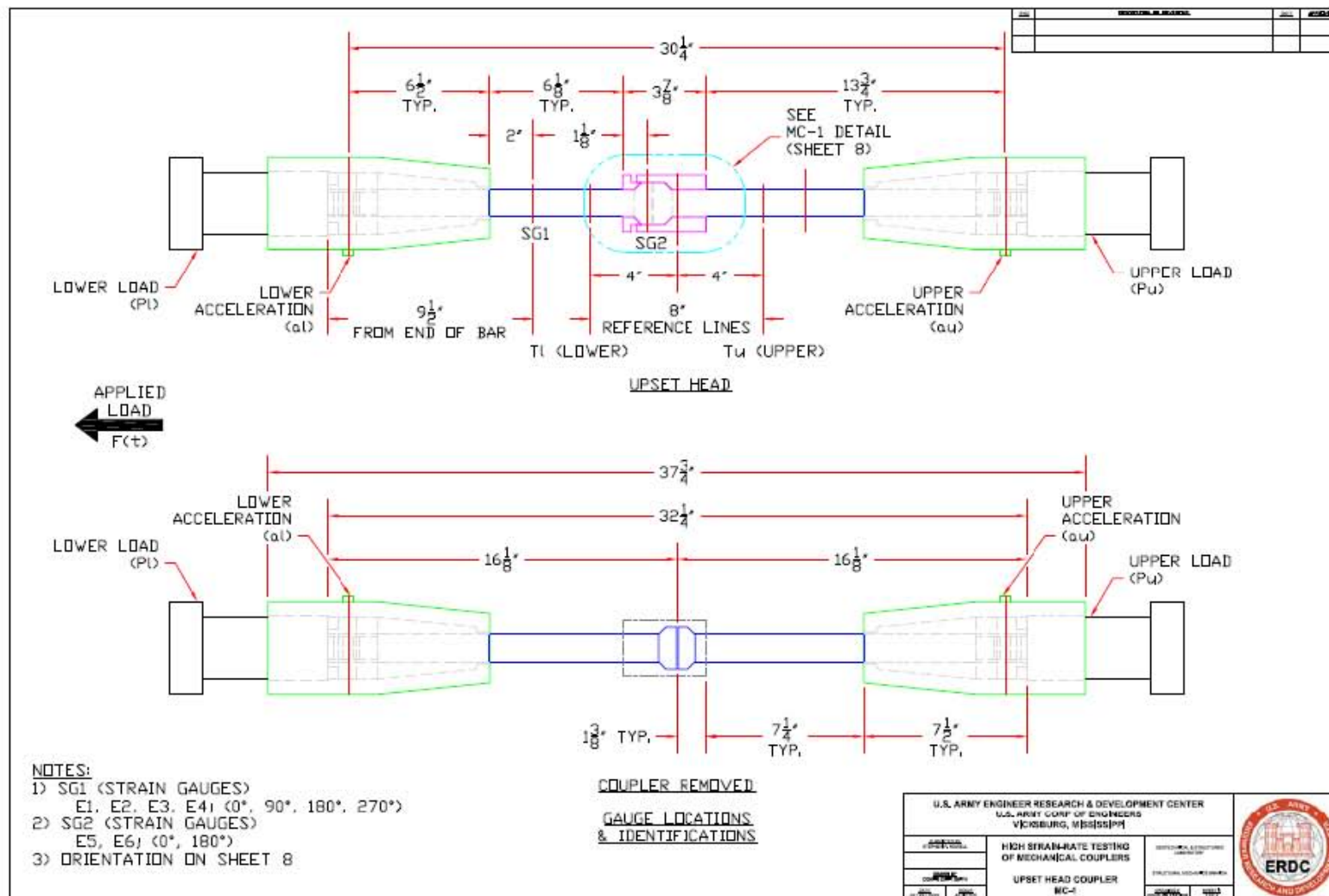Figure A1. As-rolled and machined reinforcement bars.
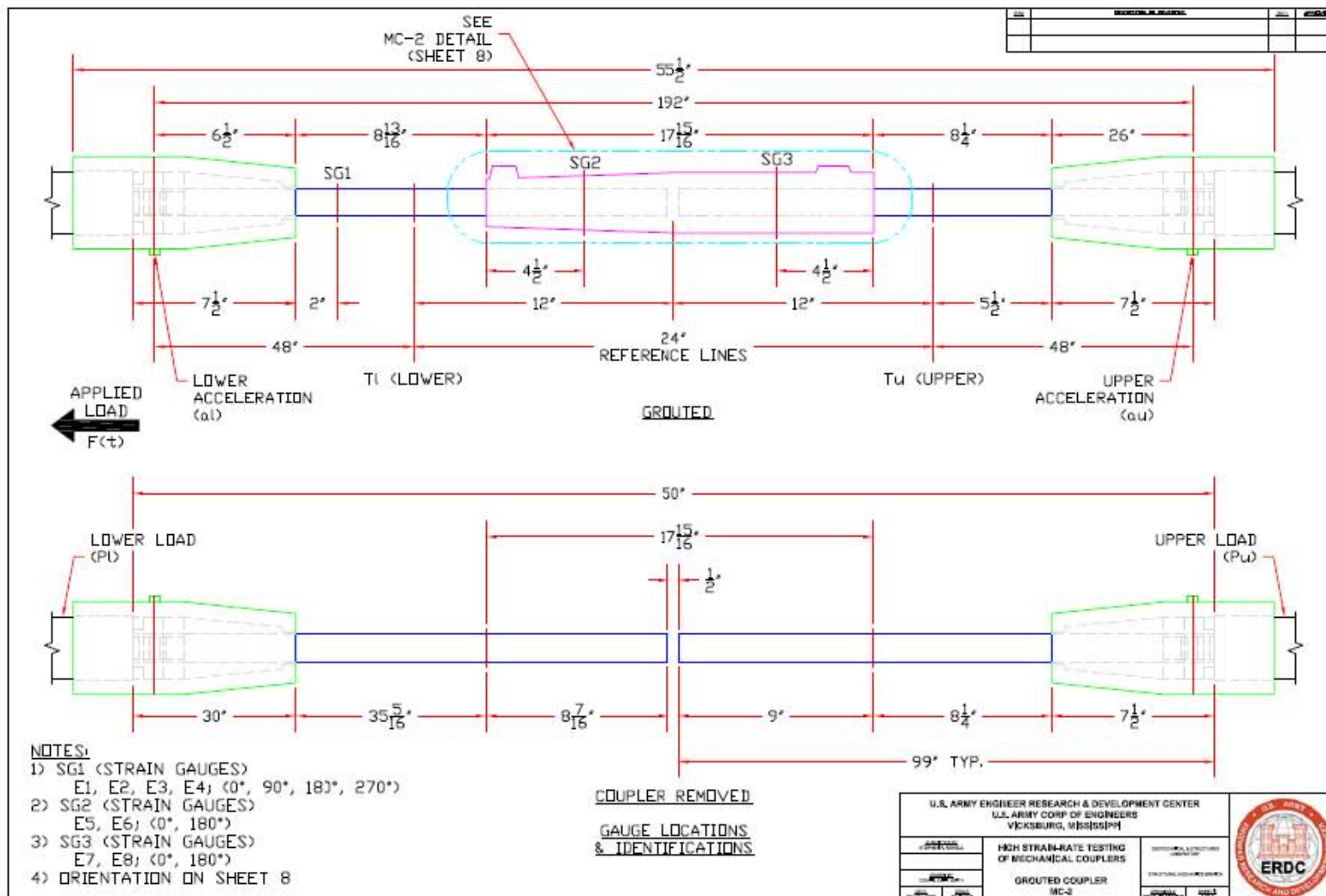
Figure A2. Upset head coupler system.

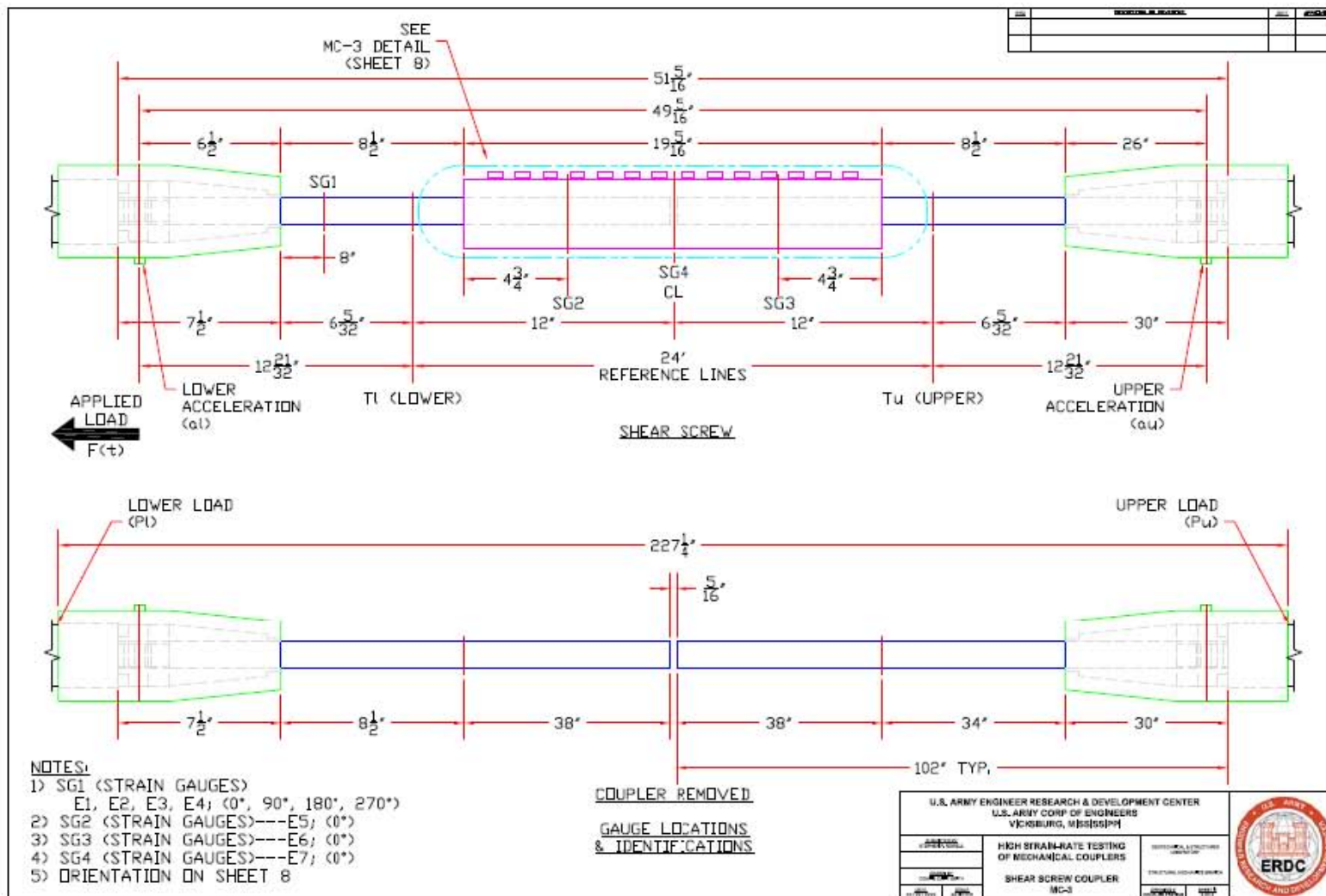Figure A3. Grouted sleeve coupler system.
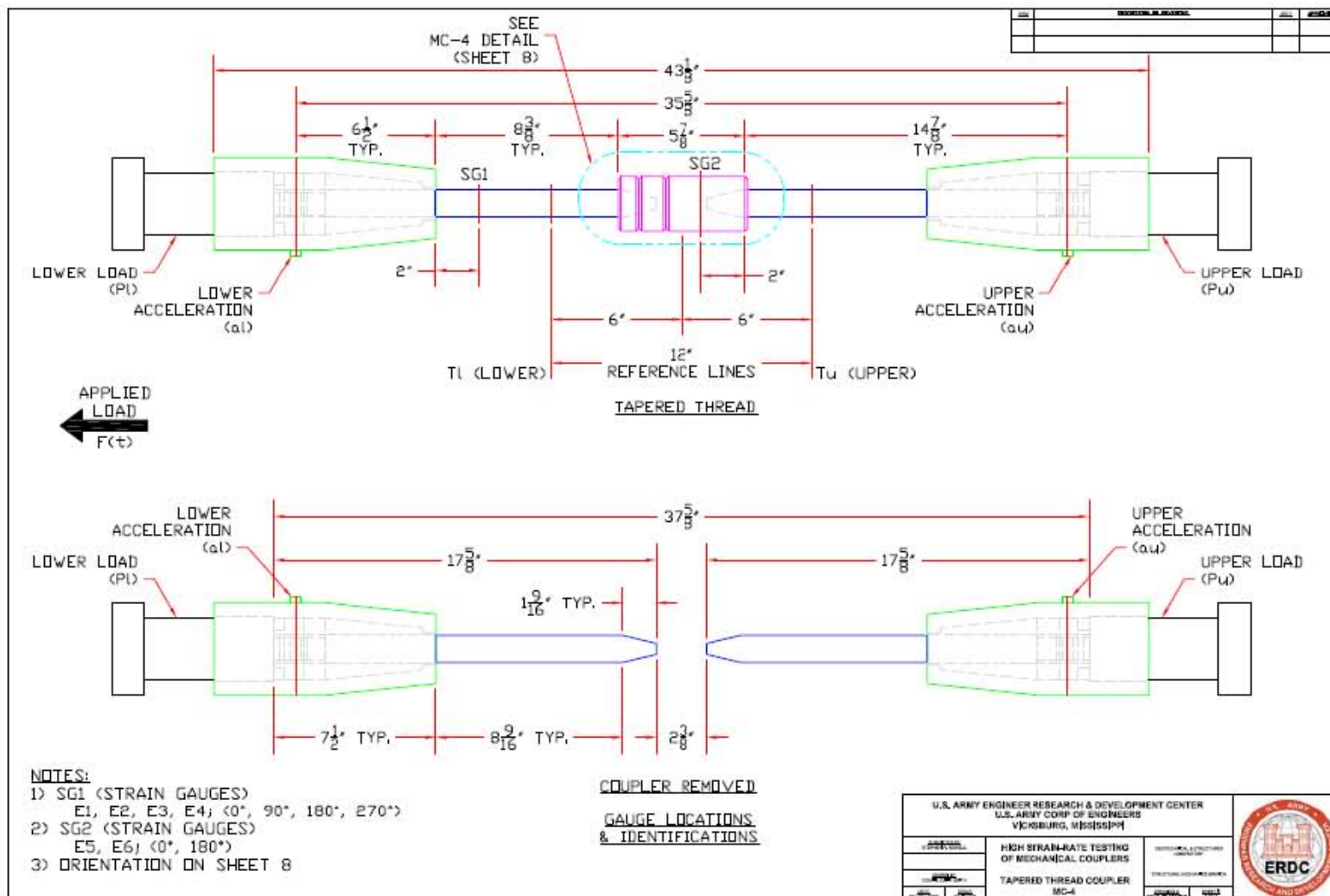
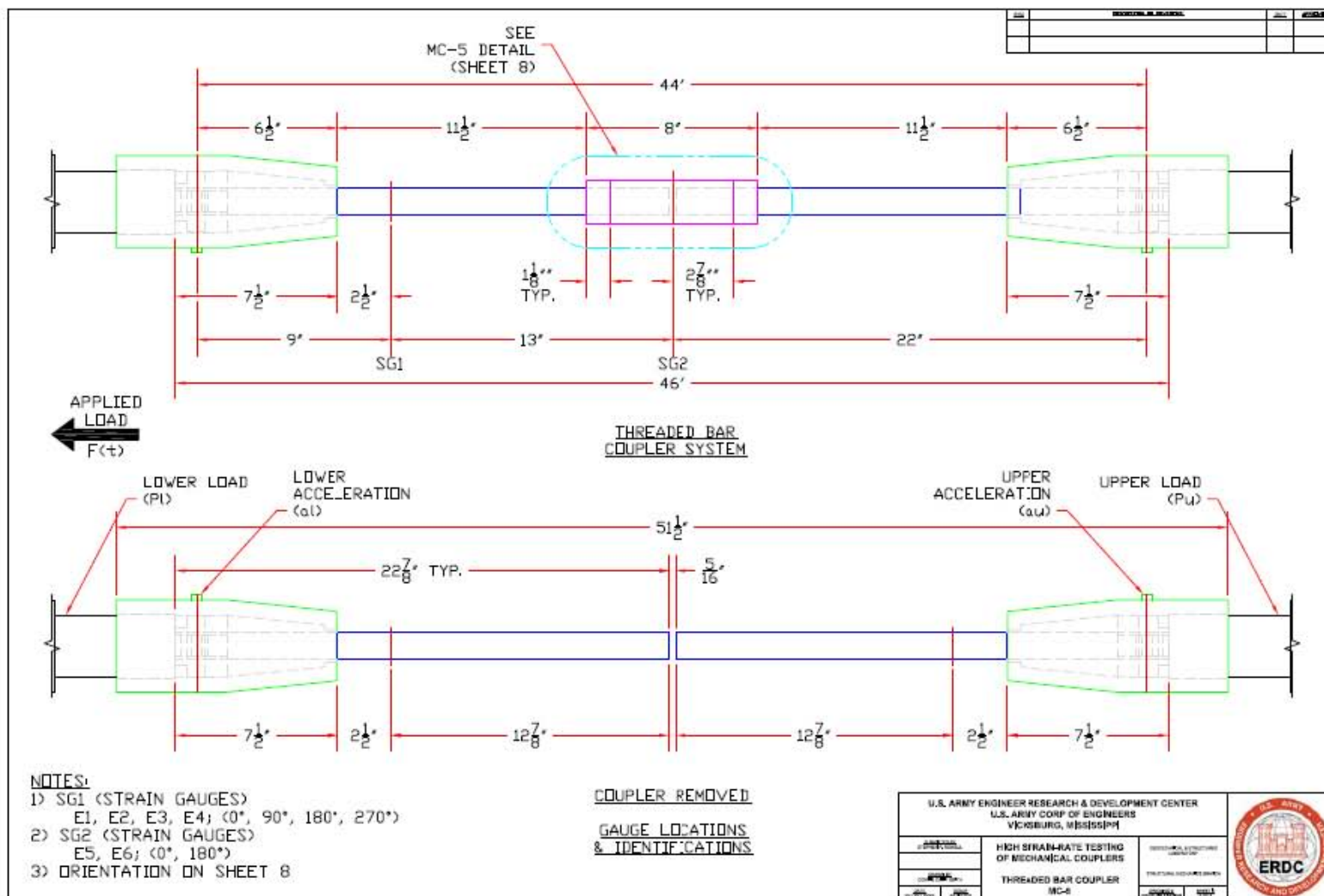Figure A4. Shear-screw coupler system.

Figure A5. Taper threaded coupler system.
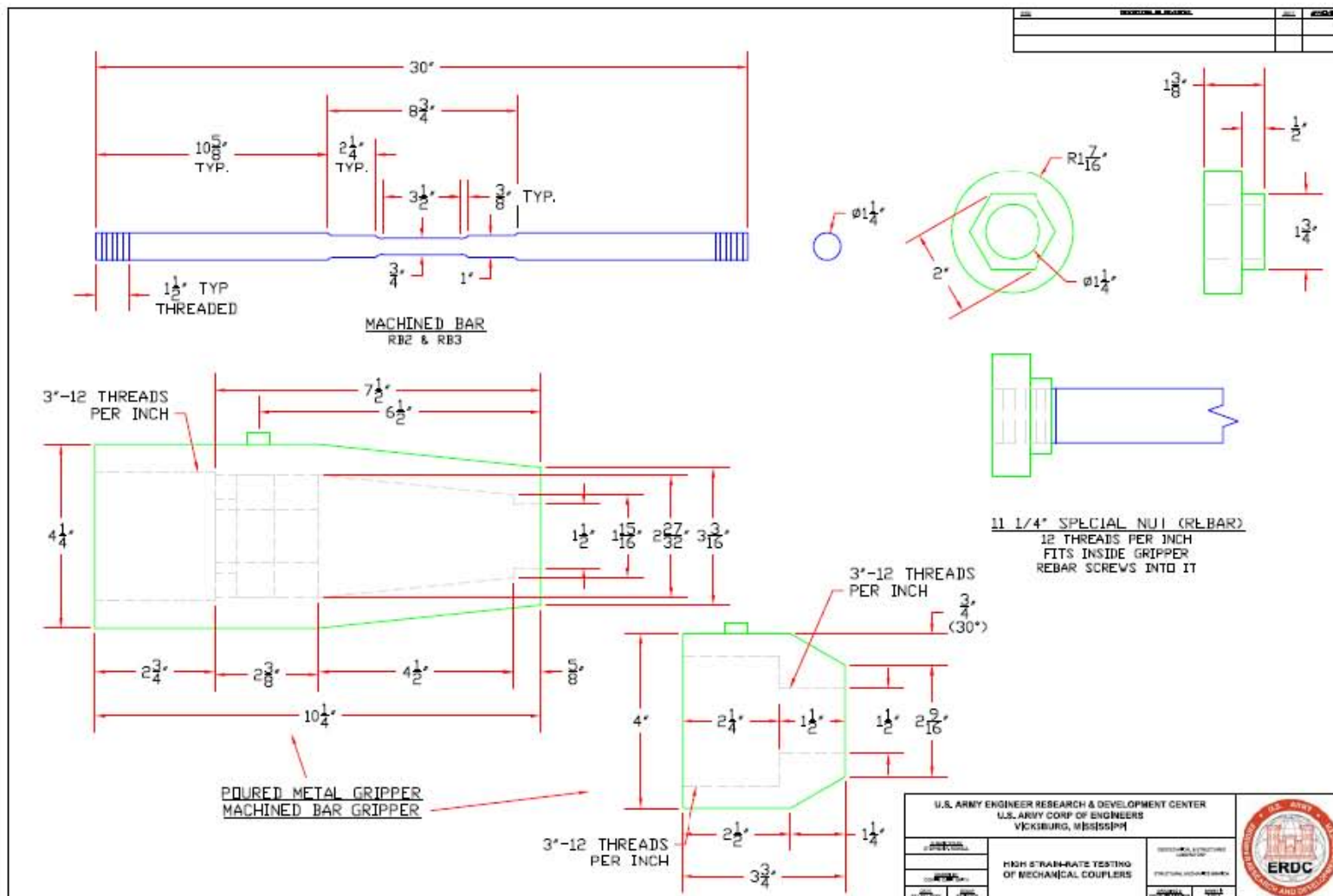
Figure A6. Threaded bar coupler system.

Figure A7. Machined bar and grip details.

Figure A8. Coupler details.
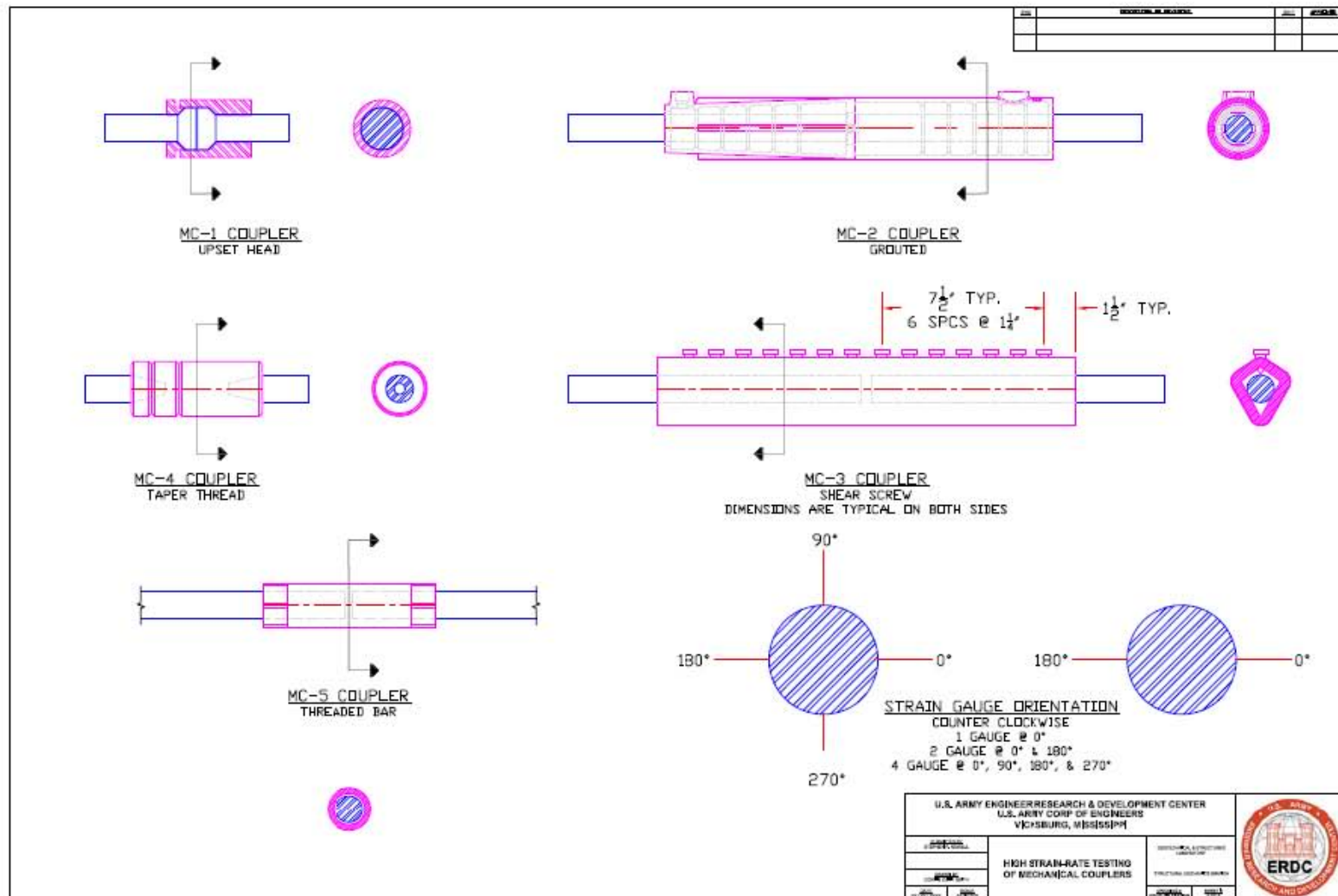
REPORT DOCUMENTATION PAGE

Public reporting burden for this collection of information is estimated to average 1 hour per response, including the time for reviewing instructions, searching existing data sources, gathering and maintaining the data needed, and completing and reviewing this collection of information. Send comments regarding this burden estimate or any other aspect of this collection of information, including suggestions for reducing this burden to Department of Defense, Washington Headquarters Services, Directorate for Information Operations and Reports (0704-0188), 1215 Jefferson Davis Highway, Suite 1204, Arlington, VA 22202-4302. Respondents should be aware that notwithstanding any other provision of law, no person shall be subject to any penalty for failing to comply with a collection of information if it does not display a currently valid OMB control number. **PLEASE DO NOT RETURN YOUR FORM TO THE ABOVE ADDRESS.**

1. REPORT DATE *(DD-MM-YYYY)*	2. REPORT TYPE	3. DATES COVERED *(From - To)*
September 2009	Final report	

4. TITLE AND SUBTITLE	5a. CONTRACT NUMBER
High Strain-Rate Testing of Mechanical Couplers	5b. GRANT NUMBER
	5c. PROGRAM ELEMENT NUMBER
6. AUTHOR(S)	5d. PROJECT NUMBER
Stephen P. Rowell, Clifford E. Grey, Stanley C. Woodson, and Kevin P. Hager	5e. TASK NUMBER
	5f. WORK UNIT NUMBER

7. PERFORMING ORGANIZATION NAME(S) AND ADDRESS(ES)	8. PERFORMING ORGANIZATION REPORT NUMBER
U.S. Army Engineer Research and Development Center Geotechnical and Structures Laboratory and Information Technology Laboratory 3909 Halls Ferry Road, Vicksburg, MS 39180-6199; Naval Facilities Engineering Service Center 1100 23rd Ave, Waterfront Structures Division Port Hueneme, CA 93043	ERDC TR-09-8

9. SPONSORING / MONITORING AGENCY NAME(S) AND ADDRESS(ES)	10. SPONSOR/MONITOR'S ACRONYM(S)
Naval Facilities Engineering Service Center Port Hueneme, CA 93043	
	11. SPONSOR/MONITOR'S REPORT NUMBER(S)

12. DISTRIBUTION / AVAILABILITY STATEMENT

Approved for public release; distribution is unlimited.

13. SUPPLEMENTARY NOTES

14. ABSTRACT

Criteria for designing structures to resist the effects of accidental explosions are defined by Army Technical Manual (TM) 5-1300. These structures are built using steel-reinforced concrete. The current practice of splicing the flexural reinforcing steel is to lap the steel, which often creates a congestion of the steel in floors, walls, and adjoining corners. In 1971, a limited number of types of splices were tested at the U.S. Army Engineer Research and Development Center (ERDC) (formerly Waterways Experiment Station) to determine their performance under dynamic load conditions. Since then, several types of mechanical couplers have been tested and validated in developing the strength of reinforcing steel for cyclic loading and at strain rates expected during earthquakes. However, no mechanical couplers have been shown to meet the TM 5-1300 requirements. Therefore, five types of these modern mechanical couplers were selected and tested at the high strain rates expected during structural response to blast loads. This report focuses on the performance of the mechanical couplers at high strain rates.

15. SUBJECT TERMS		
Concrete rebar couplers	High strain rate	Rebar splices
Dynamic material testing	Mechanical couplers	Reinforcement bar couplers

16. SECURITY CLASSIFICATION OF:			17. LIMITATION OF ABSTRACT	18. NUMBER OF PAGES	19a. NAME OF RESPONSIBLE PERSON
a. REPORT	**b. ABSTRACT**	**c. THIS PAGE**			19b. TELEPHONE NUMBER *(include area code)*
UNCLASSIFIED	UNCLASSIFIED	UNCLASSIFIED		73	